Graphical Abstract

To create your abstract, type over the instructions in the template box below.
Fonts or abstract dimensions should not be changed or altered.

Synthesis and evaluation of azalamellarin N and its A-ring-modified analogues as non-covalent inhibitors of the EGFR T790M/L858R mutant

Leave this area blank for abstract info.

Tsutomu Fukuda, Mizuho Anzai, Akane Nakahara, Kentaro Yamashita, Kazuaki Matsukura, Fumito Ishibashi, Yusuke Oku, Naoyuki Nishiya, Yoshimasa Uehara, Masatomo Iwao

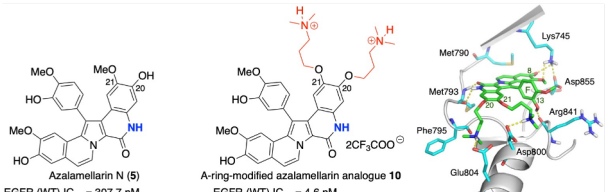

Bioorganic & Medicinal Chemistry
journal homepage: www.elsevier.com

Synthesis and evaluation of azalamellarin N and its A-ring-modified analogues as non-covalent inhibitors of the EGFR T790M/L858R mutant

Tsutomu Fukuda [a,*], Mizuho Anzai [b], Akane Nakahara [b], Kentaro Yamashita [b], Kazuaki Matsukura [c], Fumito Ishibashi [c], Yusuke Oku [d], Naoyuki Nishiya [d], Yoshimasa Uehara [d], Masatomo Iwao [b]

[a]*Environmental Protection Center, Nagasaki University, 1-14 Bunkyo-machi, Nagasaki 852-8521, Japan*
[b]*Division of Chemistry and Materials Science, Graduate School of Engineering, Nagasaki University, 1-14 Bunkyo-machi, Nagasaki 852-8521, Japan*
[c]*Division of Marine Life Science and Biochemistry, Graduate School of Fisheries and Environmental Sciences, Nagasaki University, 1-14 Bunkyo-machi, Nagasaki 852-8521, Japan*
[d]*Department of Integrated Information for Pharmaceutical Sciences, Iwate Medical University School of Pharmacy, 1-1-1 Idaidori, Yahaba-cho, Shiwa-gun, Iwate 028-3694, Japan*

ARTICLE INFO

Article history:
Received
Received in revised form
Accepted
Available online

Keywords:
EGFR tyrosine kinase inhibitors (EGFR-TKIs)
EGFR T790M/L858R mutant
Azalamellarin N
A-ring-modified azalamellarin analogues

ABSTRACT

Azalamellarin N, a synthetic lactam congener of the marine natural product lamellarin N, and its A-ring-modified analogues were synthesized and evaluated as potent and non-covalent inhibitors of the drug-resistant epidermal growth factor receptor T790M/L858R mutant. An in vitro tyrosine kinase assay indicated that the inhibitory activities of the synthetic azalamellarin analogues were higher than those of the corresponding lamellarins. The azalamellarin analogue bearing two 3-(dimethylamino)propoxy groups at C20- and C21-positions exhibited the highest activity and selectivity against the mutant kinase [IC_{50} (T790M/L858R) = 1.7 nM; IC_{50} (WT) = 4.6 nM]. The inhibitory activity was attributed to the hydrogen bonding interaction between the lactam NH group of the B-ring and carbonyl group of a methionine residue.

1. Introduction

Activating mutations in the epidermal growth factor receptor (EGFR), a member of the ErbB family of membrane tyrosine kinases, are responsible for causing a subset of non-small cell lung cancer (NSCLC).[1] Although several activating mutations have been identified, the most common mutations in NSCLC patients are the L858R point mutation and the exon 19 deletions in the kinase domain.[2] Cancer cells having such activating mutations are highly dependent on EGFR signaling for survival. Several EGFR tyrosine kinase inhibitors (EGFR-TKIs) have been developed for treating the NSCLC patients. Initially, gefitinib[3] and erlotinib[4] were found to be effective in NSCLC patients with activating EGFR mutations. These first-generation EGFR-TKIs possess a 4-anilinoquinazoline scaffold as a structural motif and act as competitive inhibitors of ATP that bind to the ATP binding pocket of the EGFR kinase domain. However, drug resistance was observed within about one year because of the T790M 'gatekeeper' mutation, which led to an increased affinity to ATP and, hence, an increased resistance to the first-generation EGFR-TKIs.[5,6] To overcome the acquired drug resistance, 4-anilinoquinazoline-based irreversible inhibitors, such as afatinib,[7] dacomitinib,[8] and neratinib[9], were developed by introducing an appropriate Michael acceptor, which could form a covalent bond with the SH group of the Cys797 residue. Although these second-generation EGFR-TKIs could effectively inhibit EGFR with activating mutations as well as those with the T790M resistance mutation, they caused serious side effects due to a total loss of selectivity between the wild-type EGFR (EGFR WT) and mutant EGFR.[10–12] Recently, pyrimidine-based irreversible inhibitors, such as WZ4002,[13] rociletinib,[14] and osimertinib[15], have been developed to target EGFRs with the T790M mutation. The affinities of these third-generation inhibitors for EGFR mutants, including T790M, are much higher than those for EGFR WT, and they exhibit a promising response to resistant NSCLC in clinical evaluations. Osimertinib was approved for the treatment of NSCLC patients harboring EGFR T790M mutation-positive tumors and, more recently, as a first-line therapy for untreated EGFR mutant NSCLC.[16] However, acquired resistance emerged despite the remarkable success of osimertinib. One of the most recognized mechanisms of osimertinib resistance and resistance to other related irreversible inhibitors was the emergence of a tertiary point mutation at Cys797, the site of covalent binding to serine (C797S).[17] Therefore, to achieve the desired potency, inhibitors of the EGFR triple mutants should be such that they do not rely on covalent bond formation with Cys797.

A marine natural product, lamellarin N (**1**), and its analogues, inhibit the catalytic activity of several protein kinases relevant to cancer and neurodegenerative diseases. These kinases include cyclin-dependent kinases (CDKs), glycogen synthase kinase-3 (GSK-3), Pim-1 proto-oncogene serine/threonine kinase (PIM1),

and dual-specificity tyrosine phosphorylation regulated kinase 1A (DYRK1A).[18,19] Recently, we designed, synthesized, and examined A-ring-modified analogues of **1** as non-covalent inhibitors of the EGFR T790M/L858R mutant and found that several water-soluble ammonium- or guanidinium-tethered analogues exhibited good inhibitory activities in the EGFR tyrosine kinase assay.[20] In particular, lamellarin-class analogue **2** bearing 3-(dimethylamino)propoxy groups at C20- and C21-positions exhibited the most potent and selective inhibition against the EGFR T790M/L858R mutant [IC_{50} (WT) = 31.8 nM; IC_{50} (T790M/L858R) = 8.9 nM] (**Fig. 1**). However, we thought that the inhibitory activity of **2** must be improved further, because the affinity of the EGFR T790M/L858R mutant to ATP is extremely high.[6] We speculated that an additional hydrogen bonding or electrostatic interaction between an amino acid residue at the ATP binding pocket of the mutant EGFR and A-ring-modified analogues of **1** could increase the affinity of the mutant EGFR to the analogues.

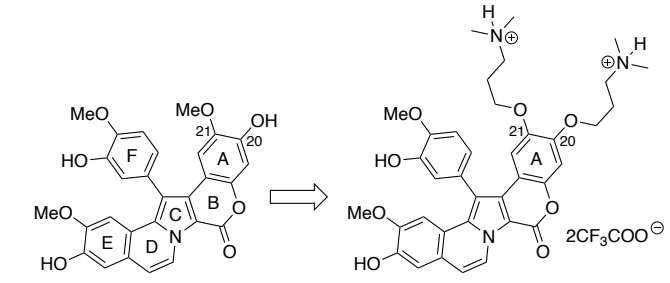

Fig. 1. Generation of lamellarin-class EGFR-TKI **2**.[20]

In 2010, Thasana and coworkers reported the synthesis and biological evaluation of a series of newly designed azalamellarins in which the lactone ring (B-ring) of lamellarins was substituted with a lactam ring.[21] Although azalamellarin D (**3**) exhibited lower cytotoxicity than lamellarin D (**4**), it maintained a high level of activity at a submicromolar range against several cancer cell lines such as HuCCA-1, A549, HepG2, and MOLT-3 (**Fig. 2**). The lactam NH moiety of **3** was considered responsible for its cytotoxicity, because N-allylated or N-propylated azalamellarin analogues were much less cytotoxic than **3**. Later, Chittchang and coworkers synthesized lamellarins N (**1**) and D (**4**) and azalamellarins N (**5**) and D (**3**) and evaluated their GSK-3β inhibitory activities (**Fig. 2**).[22] Interestingly, replacing lactone ring B with a lactam ring increased the GSK-3β inhibitory activity markedly (**1** vs **5** and **4** vs **3**); azalamellarin N (**5**) was found to be more potent than azalamellarin D (**3**). In addition, the inhibitory activity of the lamellarins against GSK-3β was dependent on the ATP concentration. However, increasing the ATP concentrations up to 1 mM did not affect the inhibitory activities of the azalamellarins, suggesting that the lactam analogues could be ATP-non-competitive inhibitors.

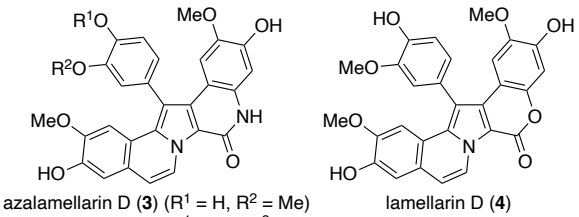

Fig. 2. Structures of azalamellarins D (**3**) and N (**5**) and lamellarin D (**4**)

Based on the abovementioned studies, we speculated that A-ring-modified azalamellarin N analogues would exhibit more potent activities against EGFR tyrosine kinases than the corresponding A-ring-modified lamellarin N analogues. In this paper, we report the synthesis and evaluation of azalamellarin N (**5**) and its A-ring-modified analogues **6–10** (**Fig. 3**).

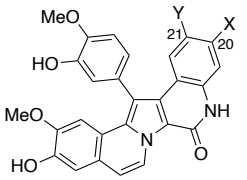

Azalamellarin	X	Y
6	OMe	OMe
7	$O(CH_2)_3N^+HMe_2$	OMe
8	$O(CH_2)_3N^+HMe_2$	OH
9	OH	$O(CH_2)_3N^+HMe_2$
10	$O(CH_2)_3N^+HMe_2$	$O(CH_2)_3N^+HMe_2$

Fig. 3. A-ring-modified azalamellarin N analogues designed to target EGFR tyrosine kinases.

2. Results and discussion

2.1. Synthesis

Recently, we successfully synthesized lamellarin N (**1**) and its A-ring-modified analogues via cross-coupling of the common tricyclic intermediate **11** (CDEF-ring of the lamellarin core) with various 2-(methoxymethoxy)phenylboronic acids bearing alkoxy functionalities at C4- and C5-positions.[20,23] Thus, we speculated that azalamellarin N and its A-ring-modified analogues **5–10** could also be accessed via a similar route for the synthesis of A-ring-modified lamellarin N analogues. Cross-coupling of **11** with 2-(*tert*-butoxycarbonylamino)phenylboronic acid pinacol esters **12** would be the key step in this synthesis (**Scheme 1**).

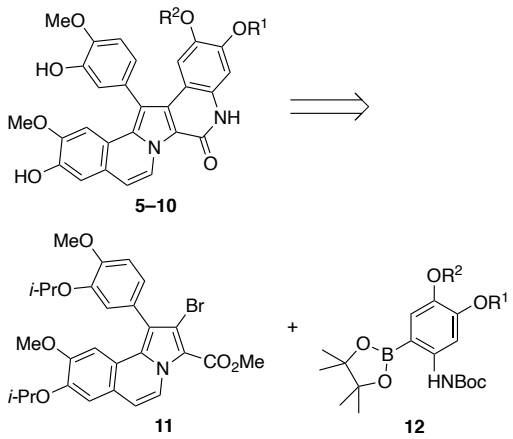

Scheme 1. Retrosynthetic analysis of azalamellarins.

The key common tricyclic intermediate **11** was synthesized in eight steps from readily available 2,5-dibromo-1-(*tert*-butoxycarbonyl)-1*H*-pyrrole (**13**) using a procedure established in our laboratories (**Scheme 2**).[20,23]

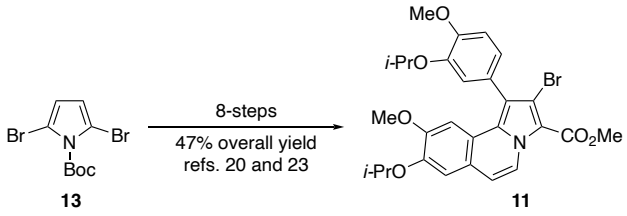

Scheme 2. Synthesis of tricyclic intermediate **11**.

Three types of 2-(*tert*-butoxycarbonylamino)phenylboronic acid pinacol esters **12a–c** were synthesized via cross-coupling of 4,5-dialkoxy-2-(*tert*-butoxycarbonylamino)phenyl bromides **14a–c** with pinacol borane (**Scheme 3**).[24] Treatment of bromides **14a–c** with 3.0 equiv of pinacol borane in the presence of

5 mol% of $PdCl_2$(dppf) and 4.0 equiv of Et_3N under reflux in 1,4-dioxane gave **12a–c** in good yields.

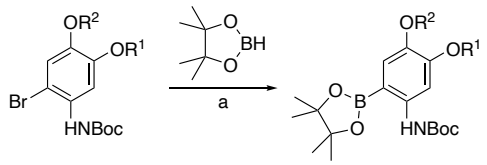

14a: R^1=Bn, R^2=Me
14b: R^1=R^2=Me
14c: R^1=R^2=Bn

12a: R^1=Bn, R^2=Me
12b: R^1=R^2=Me
12c: R^1=R^2=Bn

Scheme 3. Synthesis of arylboronic acid pinacol esters **12a–c**. *Reagents and conditions:* (a) Pd(dppf)Cl_2·CH_2Cl_2 (5 mol%), pinacol borane (3.0 equiv), Et_3N (4.0 equiv), 1,4-dioxane, reflux, 1–1.5 h (**12a**: 67%, **12b**: 84%, **12c**: 76%).

With the key common tricyclic intermediate **11** and arylboronic acid pinacol esters **12** in hand, we proceeded for the conversion to azalamellarin core (**Scheme 4**). Suzuki–Miyaura cross-coupling of **11** with **12a–c** in the presence of $Pd(PPh_3)_4$ as a catalyst gave products **15a–c** in good yields. Subsequent treatment of **15a–c** with tetrabutylammonium fluoride (TBAF) led to the removal of the N-Boc group and induced lactamization to give **16a–c** in good yields.[25]

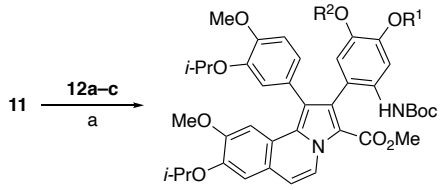

15a: R^1=Bn, R^2=Me
15b: R^1=R^2=Me
15c: R^1=R^2=Bn

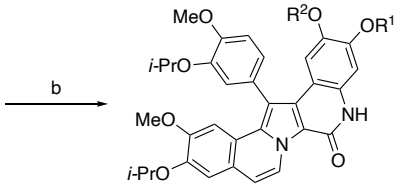

16a: R^1=Bn, R^2=Me
16b: R^1=R^2=Me
16c: R^1=R^2=Bn

Scheme 4. Synthesis of *O*-protected azalamellarins **16a–c**. *Reagents and conditions:* (a) $Pd(PPh_3)_4$ (11 mol%), **12** (1.7 equiv), Na_2CO_3 (7.3 equiv), DME, water, 85 °C, 24 h (**15a**: 91%, **15b**: 88%, **15c**: 93%); (b) TBAF (5.0 equiv), THF, 65 °C, 19 h (**16a**: 91%, **16b**: 85%, **16c**: 89%).

Next, the O-isopropyl and/or O-benzyl groups of **16a–c** were removed (**Scheme 5**). Both the isopropyl and benzyl protecting groups in **16a** and **16b** were simultaneously removed upon treatment with BCl_3 in dichloromethane (DCM) to afford fully deprotected azalamellarins **5** and **6**.[26] The spectroscopic data of compound **5** are in good agreement with the previously reported data.[22] Although we attempted the deprotection of **16c**, the desired product was not obtained. The O-benzyl groups of **16a** and **16c** could be selectively removed upon hydrogenolysis over Pd-C using HCO_2NH_4 as a hydrogen source, affording **17a** and **17b** in 99% and 97% yields, respectively.[27]

With the selectively debenzylated azalamellarins **17a** and **17b** in hand, we proceeded for their conversion to 3-(dimethylamino)propylated analogues (**Scheme 6**). When **17a** was reacted with 2 equiv of 3-(dimethylamino)propyl chloride hydrochloride in acetone in the presence of 10 equiv of K_2CO_3, compound **18** was obtained in 59% yield. Treatment of **17b** with 1.5 equiv of 3-(dimethylamino)propyl chloride hydrochloride in

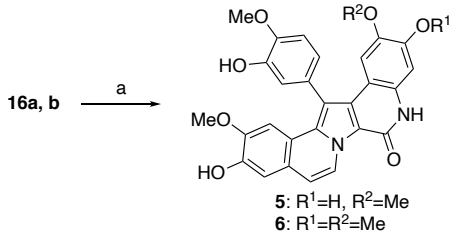

5: R^1=H, R^2=Me
6: R^1=R^2=Me

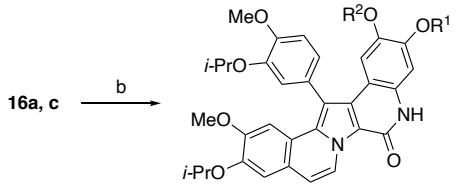

17a: R^1=H, R^2=Me
17b: R^1=R^2=H

Scheme 5. Removal of O-protecting groups. *Reagents and conditions:* (a) BCl_3, DCM, −78 °C, 0.5 h then rt, 3 h (**5**: 84%, **6**: 83%); (b) HCO_2NH_4, 10% Pd-C, EtOAc, EtOH, reflux, 0.5–1 h (**17a**: 99%, **17b**: 97%).

acetone in the presence of 6 equiv of K_2CO_3 afforded 20-O-alkylated **19**, 21-O-alkylated **20**, and 20-O,21-O-dialkylated **21** in 56%, 23%, and 4% yields, respectively, after chromatographic purification. Increasing the amounts of the alkylating agent to 2.4 equiv increased the yield of **21** to 28% and decreased the yield of **19** to 39% yield. The O-isopropyl protecting group in **18**, **19**, **20**, and **21** were easily removed upon treatment with $AlCl_3$ at room temperature for 3 d, without affecting the 3-(dimethylamino)propoxy and methoxy groups.[28] The deprotected azalamellarins **7**, **8**, **9**, and **10** were purified using a Sephadex LH-20 column and isolated as trifluoroacetate salts.

2.2. In vitro kinase assay

Kinase inhibitory activities of azalamellarins **5–10** were evaluated by enzyme-linked immunosorbent assays using the recombinant kinase domains of EGFR WT and EGFR T790M/L858R mutant.[29] Approved EGFR-TKIs, gefitinib and afatinib, were used as the positive controls. The half-maximal inhibitory concentration (IC_{50}) of the tested compounds are listed in **Table 1**. The IC_{50} values of azalamellarin N (**5**) and its 20-O-methyl analogue **6** for EGFR inhibition were in the submicromolar range, whereas the corresponding lamellarin N analogues were found to be inactive at concentrations lower than 1000 nM (entries 1 and 2).[20] Introduction of a 3-(dimethylamino)propyl group into 20-O position of **5** (i.e., compound **7**) resulted in considerably increased inhibitory activities (entry 3). The inhibitory activities of compound **8** with 21-hydroxy and 20-[3-(dimethylamino)propoxy] groups were slightly lower than those of **7** (entry 4). Transposition of the 20- and 21-substituents (X and Y) in **8** had a minor effect on the activities (entry 5). The activities of azalamellarin analogue **10** bearing 3-(dimethylamino)propoxy groups at C20- and C21-positions were higher than those of the corresponding monopropoxy azalamellarins and the corresponding lamellarin analogue **2** (entry 6). Overall, the inhibitory activities of the azalamellarins against EGFR were higher than those of the corresponding lamellarins,[20] indicating that the lactam NH group is an essential structural unit to potentiate the kinase inhibitory activities. Furthermore, inhibitory activities of all the azalamellarin analogues against EGFR T790M/L858R were higher than those against EGFR WT.

To verify whether azalamellarin compounds functioned as ATP-competitive or non-competitive inhibitors, kinase inhibition

rates were determined using azalamellarins **5**–**10** (1 μM) and three ATP concentrations (10, 100, and 1,000 μM). The results are summarized in **Table 2**. In the case of compounds **5** and **6**, the inhibition rate against EGFR WT and T790M/L858R mutant

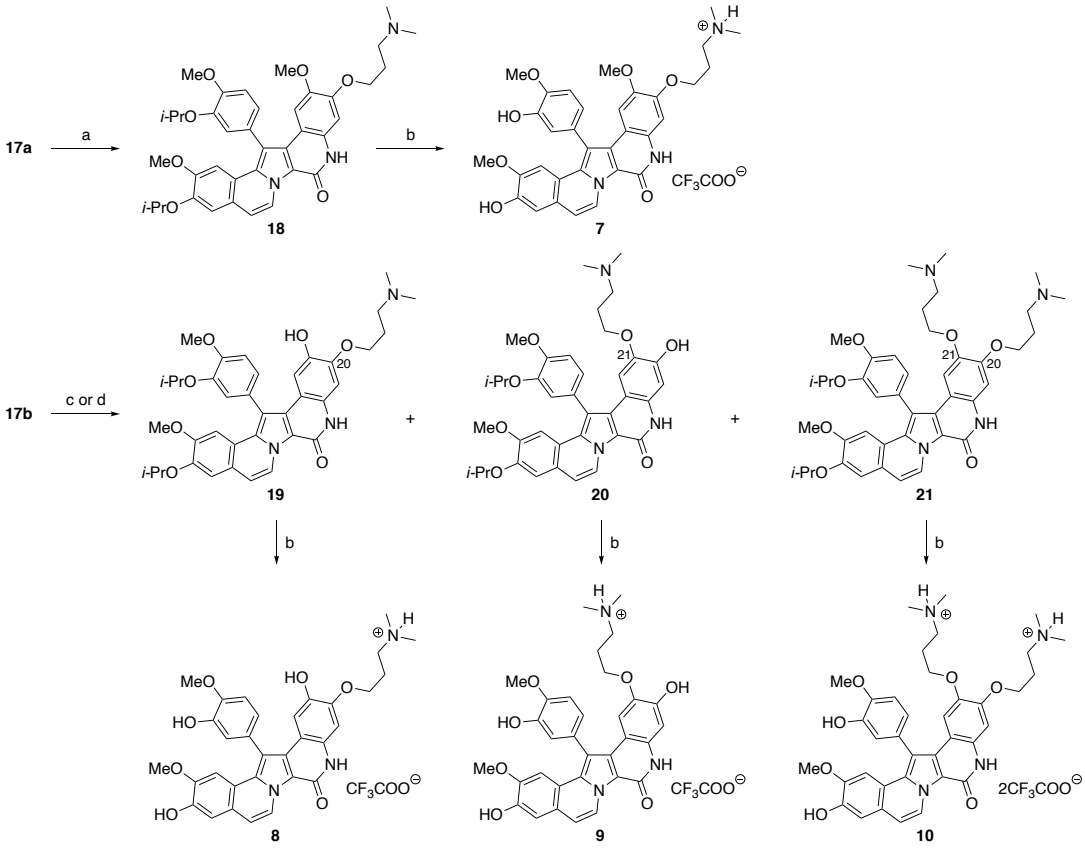

Scheme 6. Synthesis of A-ring-modified azalamellarin N analogues **7**, **8**, **9**, and **10**. *Reagents and conditions:* (a) $Cl(CH_2)_3NMe_2{\cdot}HCl$ (2.0 equiv), K_2CO_3 (10 equiv), acetone, reflux, 20 h (59%); (b) (1) $AlCl_3$, DCM, rt, 72 h, (2) TFA (**7**: quant, **8**: 94%, **9**: 95%, **10**: 97%); (c) $ClCH_2CH_2CH_2NMe_2{\cdot}HCl$ (1.5 equiv), K_2CO_3 (6.0 equiv), acetone, reflux, 22 h (**19**: 56%, **20**: 23%, **21**: 4%); (d) $Cl(CH_2)_3NMe_2{\cdot}HCl$ (2.4 equiv), K_2CO_3 (5.0 equiv), acetone, reflux, 20 h (**19**: 39%, **21**: 28%).

Table 1

Inhibitory activities of A-ring-modified azalamellarin N analogues **5**–**10** against EGFR WT and EGFR T790M/L858R mutant kinase domains.[a]

Entry	Compound	X	Y	IC_{50} (nM)	
				WT	T790M/L858R
1	**5**	OH	OMe	307.7	134.8
2	**6**	OMe	OMe	259	65.3
3	**7**	$O(CH_2)_3NMe_2 \cdot TFA$	OMe	15.5	5.7
4	**8**	$O(CH_2)_3NMe_2 \cdot TFA$	OH	24.7	10.2
5	**9**	OH	$O(CH_2)_3NMe_2 \cdot TFA$	23.6	16.6
6	**10**	$O(CH_2)_3NMe_2 \cdot TFA$	$O(CH_2)_3NMe_2 \cdot TFA$	4.6	1.7
7	gefitinib	–	–	4.0	>1000
8	afatinib	–	–	<1.0	3.8

[a] IC_{50} values were determined at an ATP concentration of 10 μM.

Table 2

Effect of ATP concentrations on the inhibition potential of azalamellarin analogues **5**–**10** against EGFR WT and EGFR T790M/L858R mutant kinase domains[a]

Compound	EGFR WT (% inhibition[b])			EGFR T790M/L858R (% inhibition[b])		
	ATP (10 μM)	ATP (100 μM)	ATP (1,000 μM)	ATP (10 μM)	ATP (100 μM)	ATP (1,000 μM)
5	79.4	18.1	4.2	88.9	18.9	5.5
6	71.5	14.1	0.6	92.7	37.8	16.9
7	83.3	19.4	4.7	99.1	69.9	0[c]
8	83.2	26.9	7.4	99.0	77.5	0[c]
9	84.9	27.8	9.1	99.1	91.5	14.3
10	87.7	33.2	12.8	97.8	84.9	13.3

[a] Inhibition rates obtained using 1 μM of azalamellarin N analogues and three concentrations of ATP (10, 100, and 1,000 μM).

[b] Percentage (%) of inhibition is represented as the mean value of two independent experiments.

[c] In case of a negative value, it was considered to be zero.

decreased proportionally to increasing ATP concentrations. In contrast, in the case of compounds **7**–**10**, the inhibition rate against EGFR T790M/L858R mutant at 100 μM ATP was maintained compared with that against EGFR WT, which was significantly low; nonetheless, the inhibition rate of both EGFR WT and T790M/L858R mutant decreased significantly at the highest ATP concentration used. Collectively, these results suggest that azalamellarin compounds can inhibit both EGFR WT and T790M/L858R mutant in an ATP-competitive manner.

2.3. Docking analysis

To rationalize the effects of B-ring moiety and A-ring-substituents X and Y on the kinase inhibitory activity, docking simulations of compounds **1**, **5**, **7**, and **10** in the ATP-binding pocket of EGFR T790M/L858R/V948R were performed using the published X-ray crystallographic data for the T790M/L858R/V948R kinase–gefitinib complex[30] [PDB ID: 4I22]. An additional V948R mutation was introduced to prevent dimerization of the T790M/L858R kinase during crystallization. This mutation had virtually no influence on the structure or activity of the T790M/L858R kinase, except the changes observed in the monomeric state in solution. Gefitinib in the ATP-binding pocket of the kinase was replaced with each ligand, and docking poses were predicted using the Autodock Vina program.[31,32] Plausible binding models and their binding affinities are represented in **Fig. 4**. In the EGFR–lamellarin N (**1**) complex model, the planar pentacyclic core (ABCDE-ring) of **1** occupied the ATP-binding pocket in such a way that the A-ring was directed to the solvent channel (entrance region) and the E-ring was oriented to the specificity (back) pocket. The F-ring, which was perpendicularly connected to the pentacyclic core, was situated at the ribose-binding site. The lactone carbonyl (C=O) group of the B-ring formed a hydrogen bond with the NH group of Met793 located in the hinge region. The phenolic OH group at C8 also formed a hydrogen bond with the side chain carboxylate group of Lys745 in the conserved catalytic salt bridge (Lys745–Asp855). Another phenolic OH at C13 of the F-ring was directed downward and formed an additional hydrogen bond with C=O of Arg841 in the A-loop. The predicted binding mode of **1** in this study was substantially similar to that reported using a different docking program.[20] The binding mode of the EGFR–azalamellarin N (**5**) complex model was similar to that of the corresponding EGFR–lamellarin N (**1**) complex model. The lactam NH group of the B-ring formed an additional hydrogen bond with C=O of Met793. This could explain the higher inhibitory activity and affinity energy of **5** compared to that of **1**. Each 3-(dimethylamino)propoxy group at the C20-position of **7** and **10** was embedded in the negatively charged small pocket in the entrance region surrounded by stem chain C=O of Phe795 and side chain carboxylate groups of both Asp800 and Glu804. The ammonium group was involved in hydrogen bonding and/or ionic interactions with the side-chain carboxylate group of Glu804. The higher activities of **10** compared to that of **7** implied that 3-(dimethylamino)propoxy group at the C21-position of **10** could form an additional hydrogen bond with Asp800. Although compounds **7** and **10** exhibited remarkably higher inhibitory activity than compounds **1** and **5**, their affinity energy was estimated to be lower than those of **1** and **5**. One possible reason for this poor correlation between activity and affinity may be attributed to the fact that **1** and **5** are neutral compounds, whereas compounds **7** and **10** are positively charged owing to their 3-(dimethylamino)propoxy group(s). Since the scoring function used in the Autodock Vina program does not explicitly consider the hydrogen atoms or partial charges for atoms,[31] it may be difficult to compare the affinity energies between uncharged and charged compounds.

2.4. Proliferation assay

Lastly, a 3-(4,5-dimethylthiazol-2-yl)-2,5-diphenyltetrazolium bromide (MTT) assay was performed to determine the effects of azalamellarin analogues **5**, **7**, and **10** on the proliferation of two kinds of NSCLC cell lines, i.e., A549 and NCI-H1975 harboring the EGFR WT and T790M/L858R mutation.[29] The IC_{50} values of the tested compounds are summarized in **Table 3**. All three compounds exhibited lower IC_{50} values in NCI-H1975 than in A549 cells, indicating that they selectively inhibited EGFR T790M/L858R rather than the WT genotype cells. Additionally, compound **5** showed markedly more potent cytotoxicity than compounds **7** and **10**, which may be caused by its multi-targeting property. Indeed, lamellarin N (**1**), the parent compound of **5**, is a potent inhibitor of topoisomerase I and a variety of protein kinases.[18,19,22]

Table 3
Cytotoxicity of azalamellarin N analogues **5**, **7**, and **10** against A549 and NCI-H1975 cells.

Compound	IC_{50} (μM)	
	A549	NCI-H1975
5	0.0155	0.0019
7	1.04	0.35
10	2.04	1.36

3. Conclusion

Azalamellarin N (**5**) and its A-ring-modified analogues **6–10** were synthesized and evaluated as non-covalent inhibitors of the EGFR T790M/L858R mutant. Analogues bearing 3-(dimethylamino)propoxy group(s) at the C20- and/or C21-position(s) exhibited good inhibitory activity against the WT and mutant EGFR, with IC_{50} values in the low, nanomolar range. In addition, azalamellarins selectively inhibited the EGFR T790M/L858R mutant over the EGFR WT and functioned as ATP-competitive inhibitors. Docking studies revealed that the higher inhibitory activities of the azalamellarin N analogues compared to the corresponding lamellarin N analogues were attributable to the additional hydrogen bonding interaction between the lactam NH group of the B-ring and C=O of Met793. Moreover, azalamellarins **5**, **7**, and **10** selectively inhibit the proliferation of EGFR T790M/L858R mutant cells over EGFR WT cells. Further biological evaluations of these azalamellarins are currently in progress in our laboratories.

4. Experimental section

4.1. Synthesis

Melting points were determined using the Yanagimoto micro melting point apparatus and are uncorrected. IR spectra were obtained with a Thermo Nicolet Nexus 670 NT FT-IR instrument and are reported in terms of the absorption frequency (cm^{-1}). NMR spectra were recorded on a JEOL JNM-AL400 instrument (400 MHz for ^1H and 100 MHz for ^{13}C) or a Varian NMR System 500PS SN instrument (500 MHz for ^1H and 126 MHz for ^{13}C). Chemical shifts for ^1H NMR are expressed in parts per million (ppm) relative to $CDCl_3$ (tetramethylsilane, δ 0.0 ppm) and DMSO-d_6 (DMSO, δ 2.50 ppm) internal standards. ^1H NMR spectral data are reported as follows: chemical shift (δ ppm), multiplicity (s = singlet, d = doublet, dd = double doublet, t = triplet, sep = septet, m = multiplet, br s = broad singlet), coupling constant (Hz), and integration. Chemical shifts for ^{13}C NMR are expressed in ppm relative to $CDCl_3$ (tetramethylsilane, δ 0.0 ppm) and DMSO-d_6 (DMSO-d_6, δ 39.52 ppm) internal standards. High-resolution mass spectra (HRMS) were recorded

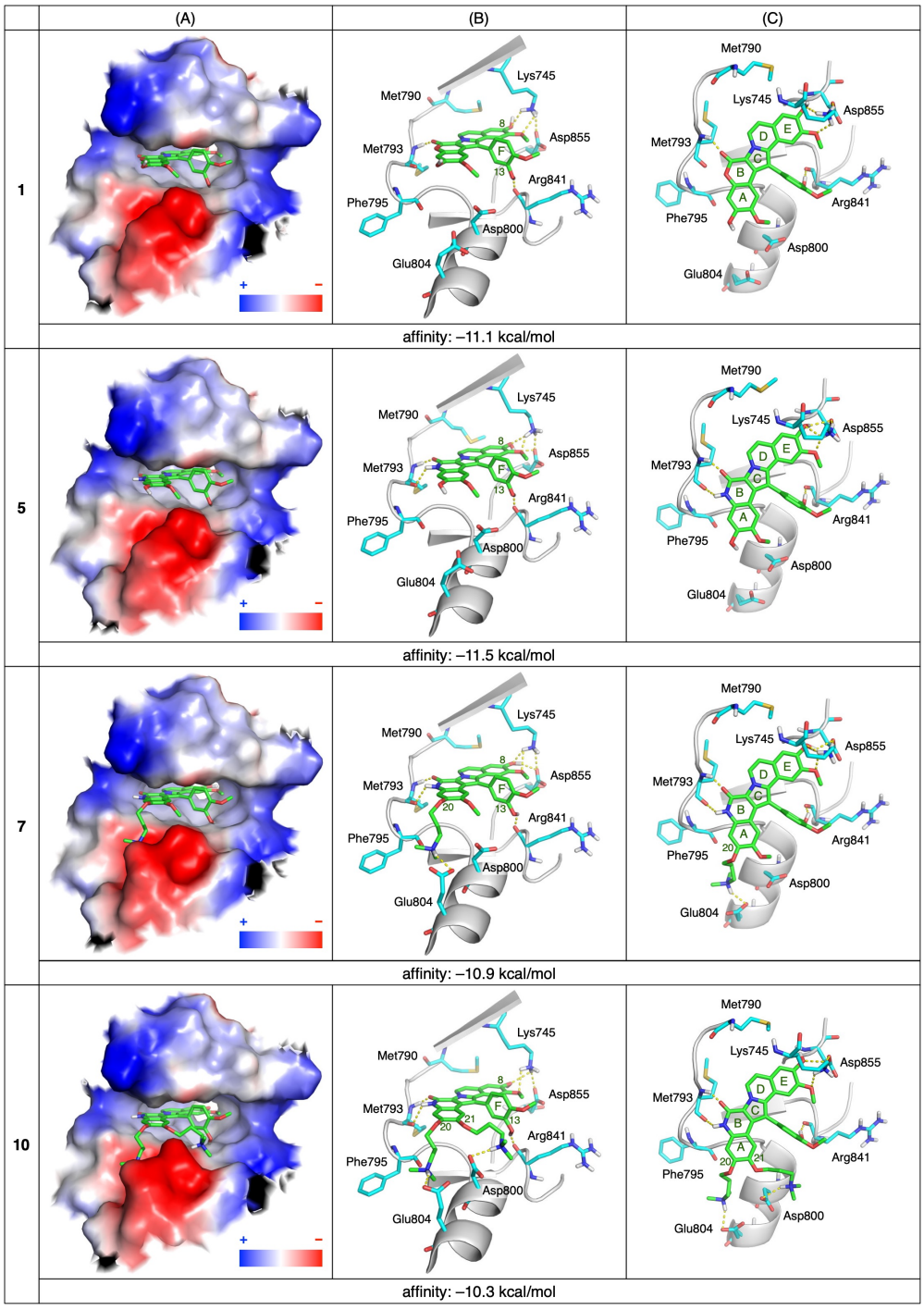

Fig. 4. Plausible binding modes of **1**, **5**, **7**, and **10** in the ATP-binding pocket of EGFR T790M/L858R/V948R. (A) Side view from the entrance region (region surrounding the ATP-binding pocket is shown by an electrostatic potential map). (B) Side view from the entrance region. (C) Top view from the N-terminal lobe.

on a JEOL JMS-T100TD (direct analysis in real-time mass spectrometry, DARTMS) instrument or a JEOL JMS-700N (fast atom bombardment mass spectrometry, FABMS) instrument. Column chromatography was performed using silica gel 60N (63–210 µm, Kanto Chemical Co., Inc.), Chromatorex Diol MB100–75/200 (Fuji Silysia Chemical Ltd.), or Sephadex LH-20 (GE Healthcare Life Sciences). Flash chromatography was performed using Chromatorex NH-DM2035 (Fuji Silysia Chemical Ltd.).

4.2. Synthesis of arylboronic acid pinacol esters ***12a–c***

*4.2.1. tert-Butyl N-[5-(benzyloxy)-4-methoxy-2-(4,4,5,5-tetramethyl-1,3,2-dioxaborolan-2-yl)phenyl]carbamate (**12a**)*

Under an argon atmosphere, a mixture of **14a** (1.01 g, 2.46 mmol), pinacol borane (1.06 mL, 7.37 mmol), $Pd(dppf)Cl_2 \cdot CH_2Cl_2$ (100 mg, 0.123 mmol), triethylamine (1.37 mL, 9.83 mmol), and 1,4-dioxane (14 mL) was refluxed for 1.5 h. After cooling to room temperature, the mixture was added saturated aqueous NH_4Cl and evaporated. The product was extracted with DCM and the extract was washed with water and brine, dried over Na_2SO_4, and evaporated. The residue was purified by column chromatography over silica gel 60N (hexane–ethyl acetate = 7:1) to give **12a** as a colorless solid (756 mg, 67%). Recrystallization from Et_2O–hexane gave colorless powder. Mp 128.5–129.5 °C. IR (KBr): 3367, 1725, 1613, 1529, 1365, 1311, 1237, 1169 cm^{-1}. ^1H NMR (400 MHz, $CDCl_3$): δ 1.35 (s, 12H), 1.52 (s, 9H), 3.86 (s, 3H), 5.19 (s, 2H), 7.18 (s, 1H), 7.27–7.32 (m, 1H), 7.33–7.39 (m, 2H), 7.47–7.51 (m, 2H),

8.02 (br s, 1H), 8.63 (br s, 1H). ^{13}C NMR (100 MHz, $CDCl_3$): δ 24.8, 28.4, 56.4, 70.4, 79.5, 83.9, 103.5, 118.3, 127.8, 127.8, 128.4, 136.7, 140.6, 143.9, 151.8, 153.2. HRDARTMS *m*/*z*. Calcd for $C_{25}H_{34}BNO_6$ (M^+): 455.2479. Found: 455.2485.

*4.2.2. tert-Butyl N-[4,5-dimethoxy-2-(4,4,5,5-tetramethyl-1,3,2-dioxaborolan-2-yl)phenyl]carbamate (**12b**)*

According to the procedure described for the preparation of **12a**, **14b** (7.18 g, 21.6 mmol), pinacol borane (9.40 mL, 65.4 mmol), and Pd(dppf)Cl_2·CH_2Cl_2 (885 mg, 1.08 mmol) were reacted for 1 h. After purification by column chromatography over silica gel 60N (hexane–ethyl acetate = 5:1), **12b** was obtained as a colorless solid (6.88 g, 84%). Recrystallization from Et_2O–hexane gave colorless powder. Mp 90–91 °C. IR (KBr): 3369, 1727, 1532, 1363, 1166, 1139 cm^{-1}. ^{1}H NMR (400 MHz, $CDCl_3$): δ 1.35 (s, 12H), 1.52 (s, 9H), 3.88 (s, 3H), 3.94 (s, 3H), 7.15 (s, 1H), 7.93 (br s, 1H), 8.67 (br s, 1H). ^{13}C NMR (100 MHz, $CDCl_3$): δ 24.9, 28.4, 55.8, 56.1, 79.6, 84.0, 101.9, 117.3, 140.8, 143.5, 152.4, 153.2. HRDARTMS *m*/*z*. Calcd for $C_{19}H_{30}BNO_6$ (M^+): 379.2166. Found: 379.2169.

*4.2.3. tert-Butyl N-[4,5-bis(benzyloxy)-2-(4,4,5,5-tetramethyl-1,3,2-dioxaborolan-2-yl)phenyl]carbamate (**12c**)*

According to the procedure described for the preparation of **12a**, **14c** (2.00 g, 4.13 mmol), pinacol borane (1.79 mL, 12.4 mmol), and Pd(dppf)Cl_2·CH_2Cl_2 (169 mg, 0.206 mmol) were reacted for 1 h. After purification by column chromatography over silica gel 60N (hexane–ethyl acetate = 7:1), **12c** was obtained as a colorless solid (1.66 g, 76%). Recrystallization from Et_2O–hexane gave colorless powder. Mp 150.5–151.5 °C. IR (KBr): 3354, 1714, 1611, 1533, 1372, 1238, 1140 cm^{-1}. ^{1}H NMR (400 MHz, $CDCl_3$): δ 1.35 (s, 12H), 1.53 (s, 9H), 5.07 (s, 2H), 5.19 (s, 2H), 7.27–7.38 (m, 6H), 7.33 (s, 1H), 7.42–7.46 (m, 2H), 7.47–7.51 (m, 2H), 8.05 (br s, 1H), 8.66 (br s, 1H). ^{13}C NMR (100 MHz, $CDCl_3$): δ 24.8, 28.4, 70.4, 72.4, 79.6, 84.0, 103.9, 123.0, 127.6, 127.6, 127.7, 128.3, 128.4, 136.9, 137.7, 141.5, 143.1, 153.1, 153.2. HRDARTMS *m*/*z*. Calcd for $C_{31}H_{38}BNO_6$ (M^+): 531.2792. Found: 531.2773.

*4.3. Synthesis of O-protected azalamellarins **16a–c***

*4.3.1. Methyl 2-[4-(benzyloxy)-2-(tert-butoxycarbonylamino)-5-methoxyphenyl]-8-isopropoxy-1-(3-isopropoxy-4-methoxyphenyl)-9-methoxy-pyrrolo[2,1-a]isoquinoline-3-carboxylate (**15a**)*

Under an argon atmosphere, a mixture of **11** (100 mg, 0.180 mmol), **12a** (137 mg, 0.302 mmol), $Pd(PPh_3)_4$ (23.2 mg, 20.1 μmol), Na_2CO_3 (141 mg, 1.33 mmol), DME (5.0 mL), and degassed water (0.5 mL) was heated in a sealed tube at 85 °C for 24 h. After cooling to room temperature, the mixture was evaporated and the product was extracted with DCM. The extract was washed with water and brine, dried over Na_2SO_4, and evaporated. The residue was purified by column chromatography over silica gel 60N (hexane–ethyl acetate = 3:1–1:2) to give **15a** as a pale yellow semisolid (131 mg, 91%). IR (KBr): 3421, 1725, 1685, 1533, 1486, 1373, 1156, 1122 cm^{-1}. ^{1}H NMR (500 MHz, DMSO-d_6): δ 1.02 (d, J = 6.1 Hz, 1.67H), 1.10 (d, J = 6.1 Hz, 1.67H), 1.13 (d, J = 6.1 Hz, 1.33H), 1.17 (d, J = 6.1 Hz, 1.33H), 1.30 (d, J = 6.1 Hz, 6H), 1.37 (s, 9H), 3.29 (s, 1.33H), 3.30 (s, 1.67H), 3.49 (s, 1.67H), 3.53 (s, 1.33H), 3.54 (s, 1.67H), 3.57 (s, 1.33H), 3.72 (s, 1.33H), 3.74 (s, 1.67H), 4.28 (sep, J = 6.1 Hz, 0.56H), 4.44 (sep, J = 6.1 Hz, 0.44H), 4.71 (sep, J = 6.1 Hz, 1H), 4.92–5.01 (m, 2H), 6.56 (s, 0.56H), 6.75 (s, 0.44H), 6.86–7.10 (m, 4H), 7.18 (d, J = 7.6 Hz, 0.56H), 7.19 (d, J = 7.6 Hz, 0.44H), 7.23–7.47 (m, 7H), 7.64 (s, 0.44H), 7.89 (s, 0.56H), 9.21 (d, J = 7.6 Hz, 0.56H), 9.23 (d, J = 7.6 Hz, 0.44H). ^{13}C NMR (126 MHz, DMSO-d_6): δ 21.5, 21.7, 21.7, 21.7, 21.7, 21.7, 21.8, 21.8, 28.1, 50.8, 50.9, 54.3, 54.4, 55.5, 55.5, 55.6, 59.7, 69.8, 70.0, 70.1, 70.1, 78.5, 78.5, 104.8, 108.2, 109.1, 110.2, 110.3, 111.7, 112.0, 112.1, 112.3, 112.4, 114.8, 115.1, 118.8, 118.8, 118.8, 118.9, 119.7, 120.4, 122.7, 122.7, 123.0, 123.0, 123.6, 124.5, 127.7, 127.9, 127.9, 128.0, 128.3, 129.9, 129.9, 130.0, 130.4, 131.0, 131.1, 137.0, 144.2, 144.3, 146.3, 146.4, 146.4, 146.4, 147.0, 147.1, 149.0, 149.1, 149.4, 149.4, 153.0, 153.3, 161.6. HRDARTMS *m*/*z*. Calcd for $C_{47}H_{53}N_2O_{10}$ [$(M+H)^+$]: 805.3700. Found: 805.3715.

*4.3.2. Methyl 2-[2-(tert-butoxycarbonylamino)-4,5-dimethoxyphenyl]-8-isopropoxy-1-(3-isopropoxy-4-methoxyphenyl)-9-methoxy-pyrrolo[2,1-a]isoquinoline-3-carboxylate (**15b**)*

According to the procedure described for the preparation of **15a**, **11** (100 mg, 0.180 mmol) and **12b** (114 mg, 0.301 mmol) were reacted. After purification by column chromatography over silica gel 60N (hexane–ethyl acetate = 3:1–1:1), **15b** was obtained as a pale yellow semisolid (115 mg, 88%). IR (KBr): 3420, 1726, 1686, 1533, 1486, 1375, 1208, 1158 cm^{-1}. ^{1}H NMR (500 MHz, DMSO-d_6): δ 1.02 (d, J = 6.1 Hz, 1.72H), 1.09 (d, J = 6.1 Hz, 1.72H), 1.11 (d, J = 6.1 Hz, 1.28H), 1.16 (d, J = 6.1 Hz, 1.28H), 1.30 (d, J = 6.1 Hz, 6H), 1.37 (s, 9H), 3.29 (s, 1.28H), 3.29 (s, 1.72H), 3.48 (s, 1.72H), 3.53 (s, 1.28H), 3.53 (s, 1.72H), 3.56 (s, 1.28H), 3.69 (s, 1.72H), 3.70 (s, 1.28H), 3.71 (s, 1.28H), 3.74 (s, 1.72H), 4.26 (sep, J = 6.1 Hz, 0.57H), 4.43 (sep, J = 6.1 Hz, 0.43H), 4.70 (sep, J = 6.1 Hz, 1H), 6.52 (s, 0.57H), 6.71 (s, 0.43H), 6.85–7.17 (m, 4H), 7.18 (d, J = 7.6 Hz, 0.57H), 7.18 (d, J = 7.6 Hz, 0.43H), 7.34 (s, 1H), 7.35 (br s, 0.43H), 7.44 (br s, 0.57H), 7.60 (br s, 0.43H), 7.85 (s, 0.57H), 9.20 (d, J = 7.6 Hz, 0.57H), 9.23 (d, J = 7.6 Hz, 0.43H). ^{13}C NMR (126 MHz, DMSO-d_6): δ 21.6, 21.7, 21.7, 21.7, 21.8, 21.8, 21.8, 25.0, 28.1, 50.8, 50.9, 54.4, 54.4, 55.2, 55.3, 55.4, 55.5, 55.5, 55.6, 69.8, 70.1, 70.1, 73.5, 78.5, 78.5, 104.8, 106.4, 107.4, 110.2, 110.3, 111.7, 112.0, 112.1, 112.3, 112.3, 112.4, 112.4, 114.6, 114.8, 118.8, 118.8, 118.9, 118.9, 118.9, 119.0, 119.7, 119.8, 122.7, 122.7, 123.0, 123.0, 123.6, 124.5, 127.7, 127.9, 128.1, 129.9, 129.9, 130.0, 130.3, 130.4, 131.1, 131.1, 134.0, 143.8, 143.9, 146.4, 146.4, 147.1, 147.1, 147.1, 147.2, 149.0, 149.1, 149.4, 153.0, 153.3, 161.6. HRDARTMS *m*/*z*. Calcd for $C_{41}H_{49}N_2O_{10}$ [$(M+H)^+$]: 729.3387. Found: 729.3358.

*4.3.3. Methyl 2-[4,5-bis(benzyloxy)-2-(tert-butoxycarbonylamino)phenyl]-8-isopropoxy-1-(3-isopropoxy-4-methoxyphenyl)-9-methoxy-pyrrolo[2,1-a]isoquinoline-3-carboxylate (**15c**)*

According to the procedure described for the preparation of **15a**, **11** (200 mg, 0.359 mmol) and **12c** (321 mg, 0.603 mmol) were reacted. After purification by column chromatography over silica gel 60N (hexane–ethyl acetate = 3:1), **15c** was obtained as a pale yellow semisolid (294 mg, 93%). IR (KBr): 3418, 1726, 1685, 1507, 1486, 1372, 1224, 1155 cm^{-1}. ^{1}H NMR (500 MHz, DMSO-d_6): δ 1.03 (d, J = 6.0 Hz, 1.65H), 1.09 (d, J = 6.0 Hz, 1.35H), 1.10 (d, J = 6.0 Hz, 1.65H), 1.15 (d, J = 6.0 Hz, 1.35H), 1.30 (d, J = 6.0 Hz, 6H), 1.37 (s, 4.95H), 1.37 (s, 4.05H), 3.30 (s, 3H), 3.48 (s, 1.35H), 3.51 (s, 1.65H), 3.71 (s, 1.35H), 3.72 (s, 1.65H), 4.28 (sep, J = 6.0 Hz, 0.55H), 4.45 (sep, J = 6.0 Hz, 0.45H), 4.70 (sep, J = 6.0 Hz, 1H), 4.72 (d, J = 12.2 Hz, 0.55H), 4.78 (d, J = 12.0 Hz, 0.45H), 4.88 (d, J = 12.2 Hz, 0.55H), 4.96 (d, J = 12.0 Hz, 0.45H), 4.97 (d, J = 11.7 Hz, 0.45H), 4.99 (d, J = 11.7 Hz, 0.55H), 5.03 (d, J = 11.7 Hz, 1H), 6.67 (s, 0.55H), 6.87–7.01 (m, 4.45H), 7.18 (d, J = 7.6 Hz, 0.55H), 7.19 (d, J = 7.6 Hz, 0.45H), 7.28–7.39 (m, 10H), 7.42–7.46 (m, 2H), 7.65 (s, 0.45H), 7.84 (s, 0.55H), 9.20 (d, J = 7.6 Hz, 0.55H), 9.23 (d, J = 7.6 Hz, 0.45H). ^{13}C NMR (126 MHz, DMSO-d_6): δ 21.6, 21.7, 21.7,

21.7, 21.8, 21.8, 21.8, 28.1, 28.1, 50.8, 50.9, 54.4, 54.4, 55.6, 55.6, 69.9, 70.1, 70.1, 70.2, 70.3, 70.8, 70.8, 78.6, 78.6, 104.8, 108.8, 109.5, 110.2, 110.3, 111.8, 112.1, 112.1, 112.3, 112.4, 117.6, 117.8, 118.7, 118.8, 118.8, 118.9, 118.9, 119.9, 120.4, 122.7, 122.7, 123.0, 123.1, 123.7, 124.4, 127.4, 127.4, 127.6, 127.7, 127.8, 127.8, 128.3, 128.3, 128.3, 129.9, 130.7, 130.8, 130.9, 131.0, 137.1, 137.2, 137.3, 137.4, 143.4, 143.5, 146.4, 146.4, 147.1, 147.1, 147.1, 149.1, 149.1, 149.5, 152.9, 153.2, 161.6, 161.6. HRDARTMS *m/z*. Calcd for $C_{53}H_{57}N_2O_{10}$ [(M+H)$^+$]: 881.4013. Found: 881.4040.

*4.3.4. 3-(Benzyloxy)-11-isopropoxy-14-(3-isopropoxy-4-methoxyphenyl)-2,12-dimethoxy-benzo[7,8]indolizino[3,2-c]quinolin-6(5H)-one (**16a**)*

Under an argon atmosphere, a mixture of **15a** (600 mg, 0.745 mmol), TBAF (1.0 M solution in THF, 3.70 mL, 3.70 mmol), and THF (30 mL) was heated in a sealed tube at 65 °C for 19 h. After cooling to room temperature, the reaction mixture was quenched with water and evaporated. The precipitate thus formed was collected by filtration, washed with water and MeOH, and dried under reduced pressure to give **16a** as a pale brown powder (458 mg, 91%). Recrystallization from DCM–hexane gave a pale brown powder. Mp 292–295 °C. IR (KBr): 1652, 1489, 1430, 1262, 1222, 1192 cm^{-1}. ^{1}H NMR (500 MHz, $CDCl_3$): δ 1.34 (d, J = 6.1 Hz, 3H), 1.34 (d, J = 6.1 Hz, 3H), 1.43 (d, J = 6.1 Hz, 3H), 1.44 (d, J = 6.1 Hz, 3H), 3.42 (s, 3H), 3.46 (s, 3H), 3.93 (s, 3H), 4.53 (sep, J = 6.1 Hz, 1H), 4.68 (sep, J = 6.1 Hz, 1H), 5.22 (s, 2H), 6.76–6.88 (m, 2H), 7.00–7.30 (m, 9H), 7.43–7.47 (m, 2H), 9.44 (br s, 1H), 11.05 (br s, 1H). ^{13}C NMR (126 MHz, $CDCl_3$): δ 21.9, 22.0, 22.0, 55.1, 55.3, 56.4, 70.8, 71.1, 71.2, 101.3, 105.7, 105.8, 110.5, 110.6, 110.7, 112.6, 112.9, 118.4, 119.3, 123.7, 124.2, 124.5, 127.4, 128.0, 128.6, 128.6, 129.4, 130.6, 132.3, 136.6, 145.2, 147.8, 148.1, 148.2, 149.8, 150.0, 156.5. HRDARTMS *m/z*. Calcd for $C_{41}H_{41}N_2O_7$ [(M+H)$^+$]: 673.2914. Found: 673.2939.

*4.3.5. 11-Isopropoxy-14-(3-isopropoxy-4-methoxyphenyl)-2,3,12-trimethoxy-benzo[7,8]indolizino[3,2-c]quinolin-6(5H)-one (**16b**)*

According to the procedure described for the preparation of **16a**, **15b** (620 mg, 0.850 mmol) was reacted to give **16b** as a pale yellow powder (430 mg, 85%). Recrystallization from DCM–hexane gave a colorless powder. Mp >300 °C. IR (KBr): 1646, 1510, 1434, 1265, 1224 cm^{-1}. ^{1}H NMR (500 MHz, $CDCl_3$): δ 1.35 (d, J = 6.1 Hz, 6H), 1.43 (d, J = 6.1 Hz, 6H), 3.45 (s, 3H), 3.47 (s, 3H), 3.96 (s, 3H), 3.99 (s, 3H), 4.54 (sep, J = 6.1 Hz, 1H), 4.69 (sep, J = 6.1 Hz, 1H), 6.90 (s, 1H), 6.94 (d, J = 7.4 Hz, 1H), 6.94 (s, 1H), 7.10 (s, 1H), 7.16 (d, J = 8.1 Hz, 1H), 7.17 (d, J = 1.7 Hz, 1H), 7.20 (s, 1H), 7.22 (dd, J = 1.7 and 8.1 Hz, 1H), 9.59 (d, J = 7.4 Hz, 1H), 10.58 (br s, 1H). ^{13}C NMR (126 MHz, $CDCl_3$): δ 21.9, 22.0, 55.1, 55.3, 56.0, 56.4, 71.2, 71.2, 98.9, 105.6, 105.8, 110.5, 110.6, 110.8, 110.9, 112.8, 112.9, 118.4, 119.3, 123.6, 124.2, 124.3, 128.8, 129.4, 130.6, 132.6, 144.8, 147.9, 148.2, 149.3, 149.9, 150.0, 156.6. HRDARTMS *m/z*. Calcd for $C_{35}H_{37}N_2O_7$ [(M+H)$^+$]: 597.2601. Found: 597.2612.

*4.3.6. 2,3-Bis(benzyloxy)-11-isopropoxy-14-(3-isopropoxy-4-methoxyphenyl)-12-methoxy-benzo[7,8]indolizino[3,2-c]quinolin-6(5H)-one (**16c**)*

According to the procedure described for the preparation of **16a**, **15c** (655 mg, 0.744 mmol) was reacted to give **16c** as a pale yellow powder (498 mg, 89%). Recrystallization from DCM–hexane gave a pale yellow powder. Mp 281.5–282.5 °C. IR (KBr): 1651, 1432, 1263, 1222, 1193 cm^{-1}. ^{1}H NMR (500 MHz, $CDCl_3$): δ 1.34 (d, J = 6.1 Hz, 3H), 1.36 (d, J = 6.1 Hz, 3H), 1.43 (d, J = 6.1 Hz, 3H), 1.43 (d, J = 6.1 Hz, 3H), 3.45 (s, 3H), 3.96 (s, 3H), 4.54 (sep, J = 6.1 Hz, 1H), 4.68 (sep, J = 6.1 Hz, 1H), 4.73 (s, 2H), 5.23 (s, 2H), 6.85 (s, 1H), 6.92 (d, J = 7.4 Hz, 1H), 7.06 (s, 1H), 7.08 (s, 1H), 7.13 (d, J = 8.3 Hz, 1H), 7.13 (d, J = 1.7 Hz, 1H), 7.16 (s, 1H), 7.17 (dd, J = 1.7 and 8.3 Hz, 1H), 7.26–7.38 (m, 8H), 7.45–7.48 (m, 2H), 9.44 (br s, 1H), 9.53 (d, J = 7.4 Hz, 1H). ^{13}C NMR (126 MHz, $CDCl_3$): δ 21.9, 21.9, 22.0, 22.1, 55.2, 56.4, 70.7, 71.1, 71.2, 71.2, 101.9, 105.8, 109.2, 110.7, 110.8, 111.0, 111.1, 112.8, 112.8, 118.3, 119.3, 123.6, 124.2, 127.2, 127.3, 127.7, 128.0, 128.4, 128.4, 128.5, 128.6, 129.2, 130.7, 132.6, 136.8, 136.9, 144.5, 147.9, 148.3, 149.1, 149.9, 150.1, 156.1. HRDARTMS *m/z*. Calcd for $C_{47}H_{45}N_2O_7$ [(M+H)$^+$]: 749.3227. Found: 749.3221.

*4.4. Removal of O-protecting groups of **16a**–**c***

*4.4.1. 3,11-Dihydroxy-14-(3-hydroxy-4-methoxyphenyl)-2,12-dimethoxy-benzo[7,8]indolizino[3,2-c]quinolin-6(5H)-one (azalamellarin N, **5**)*

To a cooled (−78 °C) solution of **16a** (30.0 mg, 44.6 μmol) in DCM (5.0 mL), was added dropwise a solution of BCl_3 in heptane (1.0 M, 0.445 mL, 0.445 mmol) under an argon atmosphere. The mixture was stirred at −78 °C for 30 min and 0 °C for 3 h. The reaction was quenched by adding saturated aqueous $NaHCO_3$ and the DCM was removed *in vacuo*. The precipitated solid was filtered, washed with water, and dried *in vacuo*. After purification by column chromatography over silica gel 60N (ethyl acetate to acetone), **5** was obtained as a colorless powder (18.6 mg, 84%). Mp >300 °C (sealed capillary) [lit.[22] Mp >290 °C]. IR (KBr): 3301, 1648, 1606, 1428, 1274, 1215 cm^{-1}. ^{1}H NMR (500 MHz, DMSO-d_6): δ 3.36 (s, 3H), 3.39 (s, 3H), 3.86 (s, 3H), 6.84 (s, 1H), 6.89 (s, 1H), 6.98–7.03 (m, 3H), 7.13 (s, 1H), 7.15 (s, 1H), 7.23 (d, J = 8.2 Hz, 1H), 9.33 (s, 1H), 9.37 (d, J = 7.4 Hz, 1H), 9.49 (s, 1H), 9.71 (s, 1H), 11.27 (s, 1H). ^{13}C NMR (126 MHz, DMSO-d_6) δ 54.5, 54.8, 56.2, 102.3, 105.4, 105.9, 108.5, 109.7, 110.4, 111.6, 112.1, 113.7, 117.7, 118.5, 122.3, 122.6, 123.9, 127.7, 128.8, 131.2, 131.4, 143.4, 147.1, 147.4, 147.7, 148.0, 155.4. HRDARTMS *m/z* Calcd for $C_{28}H_{23}N_2O_7$ [(M+H)$^+$]: 499.1505. Found: 499.1502. These physical and spectroscopic data are in good agreement with those previously reported.[22]

*4.4.2. 11-Hydroxy-14-(3-hydroxy-4-methoxyphenyl)-2,3,12-trimethoxy-benzo[7,8]indolizino[3,2-c]quinolin-6(5H)-one (**6**)*

According to the procedure described for the preparation of **5**, **16b** (20.0 mg, 33.5 μmol) and a solution of BCl_3 in heptane (1.0 M, 0.235 mL, 0.235 mmol) were reacted. After purification by column chromatography over silica gel 60N (acetone), **6** was obtained as a colorless powder (14.2 mg, 83%). Mp >300 °C (sealed capillary). IR (KBr): 3409, 1652, 1604, 1492, 1431, 1271, 1205 cm^{-1}. ^{1}H NMR (500 MHz, DMSO-d_6): δ 3.34 (s, 3H), 3.39 (s, 3H), 3.78 (s, 3H), 3.86 (s, 3H), 6.87 (s, 1H), 6.98–7.02 (m, 3H), 7.04 (d, J = 7.4 Hz, 1H), 7.14 (s, 1H), 7.16 (s, 1H), 7.23 (d, J = 8.7 Hz, 1H), 9.34 (s, 1H), 9.38 (d, J = 7.4 Hz, 1H), 9.73 (s, 1H), 11.34 (s, 1H). ^{13}C NMR (126 MHz, DMSO-d_6): δ 54.5, 54.7, 55.4, 56.2, 99.1, 105.4, 105.5, 109.2, 109.9, 110.7, 111.6, 112.3, 113.7, 117.7, 118.5, 122.3, 122.5, 123.9, 127.4, 128.7, 131.1, 131.3, 144.0, 147.5, 147.7, 147.7, 148.1, 149.0, 155.3. HRDARTMS *m/z* Calcd for $C_{29}H_{25}N_2O_7$ [(M+H)$^+$]: 513.1662. Found: 513.1676.

*4.4.3. 3-Hydroxy-11-isopropoxy-14-(3-isopropoxy-4-methoxyphenyl)-2,12-dimethoxy-benzo[7,8]indolizino[3,2-c]quinolin-6(5H)-one (**17a**)*

Under an argon atmosphere, ammonium formate (844 mg, 13.4 mmol) was added portionwise to a mixture of **16a** (300 mg, 0.446 mmol), palladium carbon (Pd: 10%, 60.0 mg), ethyl acetate (45 mL), and EtOH (45 mL) at room temperature and the mixture

was refluxed for 0.5 h. After cooling to room temperature, the mixture was passed through a pad of Celite. The filtrate was evaporated under reduced pressure. The residue was purified by column chromatography over silica gel 60N (acetone) to give **17a** as a pale yellow powder (258 mg, 99%). Recrystallization from DCM–hexane gave a pale brown powder. Mp 280–300 °C (dec) (sealed capillary). IR (KBr): 3565, 3335, 1629, 1490, 1460, 1432, 1257, 1220 cm^{-1}. ^1H NMR (500 MHz, DMSO-d_6): δ 1.22 (d, J = 6.0 Hz, 6H), 1.29 (d, J = 6.0 Hz, 6H), 3.33 (s, 3H), 3.33 (s, 3H), 3.85 (s, 3H), 4.57 (sep, J = 6.0 Hz, 1H), 4.71 (sep, J = 6.0 Hz, 1H), 6.76 (s, 1H), 6.90 (s, 1H), 7.08 (s, 1H), 7.10 (d, J = 7.5 Hz, 1H), 7.14 (d, J = 2.0 Hz, 1H), 7.14 (dd, J = 2.0 and 8.6 Hz, 1H), 7.28 (d, J = 8.6 Hz, 1H), 7.35 (s, 1H), 9.42 (d, J = 7.5 Hz, 1H), 9.51 (s, 1H), 11.31 (s, 1H). ^{13}C NMR (126 MHz, DMSO-d_6): δ 21.7, 21.7, 21.8, 54.3, 54.8, 56.0, 70.1, 70.3, 102.4, 105.2, 105.8, 108.5, 110.0, 110.7, 110.8, 112.2, 113.7, 118.4, 118.5, 122.7, 123.7, 123.9, 127.8, 128.6, 131.0, 131.4, 143.4, 147.2, 147.2, 147.7, 149.3, 150.0, 155.5. HRFABMS *m/z*. Calcd for $C_{34}H_{35}N_2O_7$ [$(M+H)^+$]: 583.2444. Found: 583.2444.

*4.4.4. 2,3-Dihydroxy-11-isopropoxy-14-(3-isopropoxy-4-methoxyphenyl)-12-methoxy-benzo[7,8]indolizino[3,2-c]quinolin-6(5H)-one (**17b**)*

According to the procedure described for the preparation of **17a**, **16c** (503 mg, 0.671 mmol), palladium carbon (Pd: 10%, 151 mg), ethyl acetate (500 mL), and EtOH (250 mL) were reacted for 1 h. After purification by column chromatography over silica gel 60N (acetone), **17b** was obtained as a pale yellow powder (371 mg, 97%). Recrystallization from acetone–hexane gave a pale brown powder. Mp >300 °C (sealed capillary). IR (KBr): 3550, 3385, 1655, 1490, 1436, 1249 cm^{-1}. ^1H NMR (500 MHz, DMSO-d_6): δ 1.20 (d, J = 6.1 Hz, 3H), 1.24 (d, J = 6.1 Hz, 3H), 1.29 (d, J = 6.1 Hz, 6H), 3.31 (s, 3H), 3.88 (s, 3H), 4.56 (sep, J = 6.1 Hz, 1H), 4.69 (sep, J = 6.1 Hz, 1H), 6.78 (s, 1H), 6.87 (s, 2H), 7.06–7.09 (m, 2H), 7.08 (dd, J = 2.0 and 8.0 Hz, 1H), 7.26 (d, J = 8.0 Hz, 1H), 7.33 (s, 1H), 8.61 (br s, 1H), 9.45 (d, J = 7.4 Hz, 1H), 9.50 (br s, 1H), 11.22 (br s, 1H). ^{13}C NMR (126 MHz, DMSO-d_6): δ 21.7, 21.7, 21.8, 21.9, 54.3, 55.7, 70.1, 70.1, 102.1, 105.1, 109.0, 109.3, 110.3, 110.6, 110.7, 112.2, 113.5, 118.2, 118.5, 122.7, 123.7, 123.8, 127.5, 128.5, 130.4, 131.1, 141.0, 146.4, 147.1, 147.6, 149.2, 149.9, 155.4. HRDARTMS *m/z*. Calcd for $C_{33}H_{33}N_2O_7$ [$(M+H)^+$]: 569.2288. Found: 569.2299.

*4.5. Synthesis of A-ring-modified azalamellarin N analogues **7**, **8**, **9**, and **10***

*4.5.1. 3-[3-(Dimethylamino)propoxy]-11-isopropoxy-14-(3-isopropoxy-4-methoxyphenyl)-2,12-dimethoxy-benzo[7,8]indolizino[3,2-c]quinolin-6(5H)-one (**18**)*

Under an argon atmosphere, a mixture of **17a** (117 mg, 0.201 mmol), 3-(dimethylamino)propyl chloride hydrochloride (63.6 mg, 0.402 mmol), K_2CO_3 (278 mg, 2.01 mmol), and acetone (25 mL) was refluxed for 20 h. After cooling to room temperature, the mixture was passed through a pad of Celite. The filtrate was evaporated under reduced pressure. The residue was purified by column chromatography over Chromatorex Diol MB100–75/200 (ethyl acetate to DCM–MeOH = 10:1 to 1:1) to give **18** as a pale brown solid (78.8 mg, 59%). Recrystallization from DCM–hexane gave a pale brown powder. Mp 150–180 °C (dec) (sealed capillary). IR (KBr): 1652, 1452, 1430, 1260, 1223 cm^{-1}. ^1H NMR (500 MHz, $CDCl_3$): δ 1.35 (d, J = 6.1 Hz, 6H), 1.43 (d, J = 6.1 Hz, 6H), 2.08 (quin, J = 6.9 Hz, 2H), 2.28 (s, 6H), 2.51 (t, J = 7.2 Hz, 2H), 3.45 (s, 6H), 3.96 (s, 3H), 4.17 (t, J = 6.7 Hz, 2H), 4.54 (sep, J = 6.1 Hz, 1H), 4.68 (sep, J = 6.1 Hz, 1H), 6.88 (s, 1H), 6.93 (d, J = 7.4 Hz, 1H), 7.00 (s, 1H), 7.09 (s, 1H), 7.14 (d, J = 8.2 Hz, 1H), 7.16 (d, J = 1.7 Hz, 1H), 7.19 (s, 1H), 7.21 (dd, J = 1.7 and 8.2 Hz, 1H), 9.59 (d, J = 7.4 Hz, 1H), 10.86 (br s, 1H). ^{13}C NMR (126 MHz, $CDCl_3$): δ 22.0, 22.0, 22.0, 27.3, 45.5, 55.2, 55.4, 56.3, 56.5, 67.4, 71.2, 71.3, 100.4, 105.8, 105.9, 110.5, 110.7, 110.8, 110.9, 112.8, 112.9, 118.4, 119.4, 123.7, 124.2, 124.4, 128.9, 129.5, 130.7, 132.5, 145.1, 147.9, 148.2, 148.7, 149.9, 150.0, 156.7. HRDARTMS *m/z*. Calcd for $C_{39}H_{46}N_3O_7$ [$(M+H)^+$]: 668.3336. Found: 668.3352.

*4.5.2. Trifluoroacetic acid salt of 3-[3-(dimethylamino)propoxy]-11-hydroxy-14-(3-hydroxy-4-methoxyphenyl)-2,12-dimethoxy-benzo[7,8]indolizino[3,2-c]quinolin-6(5H)-one (**7**)*

Under an argon atmosphere, a nitrobenzene solution of $AlCl_3$ (1.0 M, 145 µL, 0.145 mmol) was added dropwise to a solution of **18** (15.2 mg, 22.8 µmol) in DCM (5.0 mL) at room temperature. After stirring for 72 h at room temperature, a solution of $NaHCO_3$ (36.7 mg, 0.437 mmol) and Rochelle salt (123 mg, 0.437 mmol) in water (2.1 mL) was added. The mixture was stirred for an additional 1 h and then evaporated. The nitrobenzene was removed azeotropically with water under reduced pressure. To the residue was added DCM (1.0 mL) and TFA (1.0 mL) and then the mixture was evaporated. The residue was purified by column chromatography over Sephadex LH-20 using following solvent systems (water containing 0.1% TFA, water–MeOH = 1:1 containing 0.1% TFA, and MeOH containing 0.1% TFA) to give **7** as a brown powder (15.8 mg, quant). Mp 125–155 °C (dec) (sealed capillary). IR (KBr): 3128, 1681, 1457, 1432, 1276, 1199 cm^{-1}. ^1H NMR (500 MHz, DMSO-d_6): δ 2.14 (dt, J = 6.0 and 15.3 Hz, 2H), 2.82 (s, 3H), 2.83 (s, 3H), 3.20–3.26 (m, 2H), 3.36 (s, 3H), 3.39 (s, 3H), 3.86 (s, 3H), 4.05 (t, J = 5.9 Hz, 2H), 6.90 (s, 1H), 6.98–7.02 (m, 3H), 7.05 (d, J = 7.5 Hz, 1H), 7.14 (s, 1H), 7.16 (s, 1H), 7.23 (d, J = 8.7 Hz, 1H), 9.37 (d, J = 7.5 Hz, 1H), 9.60 (br s, 1H), 9.75 (br s, 2H), 11.37 (s, 1H). ^{13}C NMR (126 MHz, DMSO-d_6): δ 23.9, 42.4, 54.5, 54.8, 56.2, 65.8, 100.6, 105.4, 105.7, 109.8, 109.9, 110.8, 111.6, 112.4, 113.7, 117.7, 118.5, 122.2, 122.5, 123.9, 127.3, 128.6, 131.0, 131.3, 144.1, 147.5, 147.7, 147.8, 147.8, 148.1, 155.3. HRDARTMS *m/z*. Calcd for $C_{33}H_{34}N_3O_7$ [$(M–CF_3COO)^+$]: 584.2397. Found: 584.2381.

*4.5.3. Treatment of **17b** with 3-(dimethylamino)propyl chloride hydrochloride*

Method 1: Under an argon atmosphere, a mixture of **17b** (371 mg, 0.653 mmol), 3-(dimethylamino)propyl chloride hydrochloride (155 mg, 0.979 mmol), K_2CO_3 (541 mg, 3.92 mmol), and acetone (350 mL) was refluxed for 22 h. After cooling to room temperature, the mixture was passed through a pad of Celite. The filtrate was evaporated under reduced pressure. The residue was purified by flash chromatography over Chromatorex NH-DM2035 (DCM–MeOH = 99:1 to 97:3 to 9:1) to give **19** as a pale brown solid (237 mg, 56%), **20** as a pale brown solid (99.3 mg, 23%), and **21** as a pale brown solid (17.4 mg, 4%).

Method 2: Under an argon atmosphere, a mixture of **17b** (50.0 mg, 87.9 µmol), 3-(dimethylamino)propyl chloride hydrochloride (33.4 mg, 0.211 mmol), K_2CO_3 (60.8 mg, 0.440 mmol), and acetone (50 mL) was refluxed for 20 h. After cooling to room temperature, the mixture was passed through a pad of Celite. The filtrate was evaporated under reduced pressure. The residue was purified by column chromatography over Chromatorex Diol MB100–75/200 (DCM–MeOH = 20:1 to 10:1) to give **19** as a pale brown solid (22.2 mg, 39%) and **21** as a pale brown solid (17.9 mg, 28%).

*4.5.3.1. 3-[3-(Dimethylamino)propoxy]-2-hydroxy-11-isopropoxy-14-(3-isopropoxy-4-methoxyphenyl)-12-methoxy-benzo[7,8]indolizino[3,2-c]quinolin-6(5H)-one (**19**)*

Recrystallization from DCM–hexane gave a pale green powder. Mp 180–200 °C (dec) (sealed capillary). IR (KBr): 1650, 1449, 1434, 1259, 1219, 1188 cm^{-1}. ^1H NMR (500 MHz, $CDCl_3$): δ 1.33 (d, J = 6.1 Hz, 3H), 1.38 (d, J = 6.1 Hz, 3H), 1.42 (d, J = 6.1 Hz, 3H), 1.42 (d, J = 6.1 Hz, 3H), 1.93–2.01 (m, 2H), 2.32 (s, 6H), 2.59 (t, J = 5.6 Hz, 2H), 3.43 (s, 3H), 3.98 (s, 3H), 4.01–4.07 (m, 2H), 4.55 (sep, J = 6.1 Hz, 1H), 4.67 (sep, J = 6.1 Hz, 1H), 6.93 (d, J = 7.4 Hz, 1H), 6.99 (s, 1H), 7.03 (s, 1H), 7.04 (s, 1H), 7.07 (s, 1H), 7.10–7.18 (m, 3H), 9.60 (d, J = 7.4 Hz, 1H), 9.89 (br s, 1H). ^{13}C NMR (126 MHz, $CDCl_3$): δ 21.9, 21.9, 22.1, 26.4, 44.9, 55.1, 56.2, 57.4, 71.1, 71.1, 72.5, 105.8, 107.0, 110.7, 110.8, 111.0, 111.5, 112.9, 113.1, 118.4, 119.4, 123.7, 124.1, 124.2, 128.2, 129.0, 129.0, 132.6, 145.8, 147.3, 147.7, 148.2, 149.8, 150.2, 156.3. HRDARTMS *m*/*z*. Calcd for $C_{38}H_{44}N_3O_7$ [(M+H)$^+$]: 654.3179. Found: 654.3175.

*4.5.3.2. 2-[3-(Dimethylamino)propoxy]-3-hydroxy-11-isopropoxy-14-(3-isopropoxy-4-methoxyphenyl)-12-methoxy-benzo[7,8]indolizino[3,2-c]quinolin-6(5H)-one (**20**)*

Recrystallization from DCM–hexane gave a pale brown powder. Mp 170–200 °C (dec) (sealed capillary). IR (KBr): 1650, 1488, 1451, 1432, 1259, 1220 cm^{-1}. ^1H NMR (500 MHz, $CDCl_3$): δ 1.35 (d, J = 6.1 Hz, 3H), 1.38 (d, J = 6.1 Hz, 3H), 1.43 (d, J = 6.1 Hz, 6H), 1.82–1.93 (m, 2H), 2.36 (s, 6H), 2.55–2.64 (m, 2H), 3.44 (s, 3H), 3.72–3.82 (m, 2H), 3.99 (s, 3H), 4.56 (sep, J = 6.1 Hz, 1H), 4.68 (sep, J = 6.1 Hz, 1H), 6.88 (s, 1H), 6.93 (d, J = 7.4 Hz, 1H), 7.03 (s, 1H), 7.08 (s, 2H), 7.14 (d, J = 1.6 Hz, 1H), 7.14 (d, J = 8.2 Hz, 1H), 7.17 (dd, J = 1.6 and 8.2 Hz, 1H), 9.57 (d, J = 7.4 Hz, 1H), 9.92 (br s, 1H). ^{13}C NMR (126 MHz, $CDCl_3$): δ 21.9, 22.0, 22.0, 26.2, 44.9, 55.1, 56.3, 57.7, 71.1, 71.1, 73.4, 103.1, 105.7, 109.4, 110.6, 110.7, 110.8, 112.4, 112.8, 115.7, 118.3, 119.3, 123.9, 124.3, 124.3, 128.8, 129.4, 132.5, 133.9, 143.2, 147.7, 148.1, 149.7, 149.9, 151.5, 156.6. HRFABMS *m*/*z*. Calcd for $C_{38}H_{44}N_3O_7$ [(M+H)$^+$]: 654.3179. Found: 654.3178.

*4.5.3.3. 2,3-Bis[3-(dimethylamino)propoxy]-11-isopropoxy-14-(3-isopropoxy-4-methoxyphenyl)-12-methoxy-benzo[7,8]indolizino[3,2-c]quinolin-6(5H)-one (**21**)*

Recrystallization from DCM–hexane gave a brown needles. Mp 165–200 °C (dec) (sealed capillary). IR (KBr): 3440, 1650, 1434, 1260, 1223, 1199 cm^{-1}. ^1H NMR (500 MHz, $CDCl_3$): δ 1.33 (d, J = 6.1 Hz, 3H), 1.33 (d, J = 6.1 Hz, 3H), 1.43 (d, J = 6.1 Hz, 6H), 1.84 (quin, J = 6.9 Hz, 2H), 2.06 (quin, J = 6.8 Hz, 2H), 2.29 (s, 6H), 2.32 (s, 6H), 2.38–2.48 (m, 2H), 2.54–2.61 (m, 2H), 3.43 (s, 3H), 3.59 (t, J = 6.3 Hz, 2H), 3.95 (s, 3H), 4.08–4.20 (m, 2H), 4.52 (sep, J = 6.1 Hz, 1H), 4.68 (sep, J = 6.1 Hz, 1H), 6.86 (s, 1H), 6.92 (s, 1H), 6.93 (d, J = 7.3 Hz, 1H), 7.08 (d, J = 8.3 Hz, 1H), 7.09 (s, 1H), 7.12 (d, J = 1.6 Hz, 1H), 7.15 (dd, J = 1.6 and 8.3 Hz, 1H), 7.16 (s, 1H), 9.54 (d, J = 7.3 Hz, 1H), 10.10 (br s, 1H). ^{13}C NMR (126 MHz, $CDCl_3$): δ 21.9, 21.9, 22.0, 22.1, 27.2, 27.3, 45.4, 45.4, 55.1, 56.3, 56.4, 66.8, 67.3, 71.2, 71.2, 100.7, 105.8, 107.7, 110.6, 110.6, 110.7, 110.9, 112.7, 112.8, 118.5, 119.3, 123.6, 124.2, 124.3, 128.7, 129.3, 130.6, 132.5, 144.3, 147.8, 148.2, 149.1, 149.9, 150.1, 156.3. HRDARTMS *m*/*z*. Calcd for $C_{43}H_{55}N_4O_7$ [(M+H)$^+$]: 739.4071. Found: 739.4045.

*4.5.4. Trifluoroacetic acid salt of 3-[3-(dimethylamino)propoxy]-2,11-dihydroxy-14-(3-hydroxy-4-methoxyphenyl)-12-methoxy-benzo[7,8]indolizino[3,2-c]quinolin-6(5H)-one (**8**)*

According to the procedure described for the preparation of **7**, **19** (14.3 mg, 21.9 μmol) and $AlCl_3$ (1.0 M solution in nitrobenzene, 162 μL, 0.162 mmol) were reacted. After purification by column chromatography over Sephadex LH-20 using following solvent systems (water containing 0.1% TFA, water–MeOH = 1:1 containing 0.1% TFA, and MeOH containing 0.1% TFA), **8** was obtained as a brown powder (14.1 mg, 94%). Mp 230–260 °C (dec) (sealed capillary). IR (KBr): 3115, 1683, 1436, 1277, 1205, 1130 cm^{-1}. ^1H NMR (500 MHz, DMSO-d_6): δ 2.14 (dt, J = 5.8 and 15.2 Hz, 2H), 2.82 (s, 3H), 2.83 (s, 3H), 3.27–3.33 (m, 2H), 3.37 (s, 3H), 3.90 (s, 3H), 4.06 (t, J = 5.7 Hz, 2H), 6.89 (s, 1H), 6.89 (s, 1H), 6.92–6.96 (m, 2H), 6.98 (s, 1H), 7.02 (d, J = 7.5 Hz, 1H), 7.12 (s, 1H), 7.22 (d, J = 8.0 Hz, 1H), 8.66 (br s, 1H), 9.35 (br s, 1H), 9.41 (d, J = 7.5 Hz, 1H), 9.64 (br s, 2H), 11.29 (s, 1H). ^{13}C NMR (126 MHz, DMSO-d_6): δ 23.8, 42.4, 54.4, 54.4, 55.9, 65.6, 100.3, 105.3, 109.4, 110.2, 110.4, 110.7, 111.6, 112.3, 113.6, 117.7, 118.3, 122.1, 122.5, 123.9, 126.9, 128.6, 130.1, 131.5, 141.6, 147.1, 147.3, 147.6, 147.7, 148.0, 155.3. HRDARTMS *m*/*z*. Calcd for $C_{32}H_{32}N_3O_7$ [(M−CF_3COO)$^+$]: 570.2240. Found: 570.2216.

*4.5.5. Trifluoroacetic acid salt of 2-[3-(dimethylamino)propoxy]-3,11-dihydroxy-14-(3-hydroxy-4-methoxyphenyl)-12-methoxy-benzo[7,8]indolizino[3,2-c]quinolin-6(5H)-one (**9**)*

According to the procedure described for the preparation of **7**, **20** (10.8 mg, 16.5 μmol) and $AlCl_3$ (1.0 M solution in nitrobenzene, 122 μL, 0.122 mmol) were reacted. After purification by column chromatography over Sephadex LH-20 using following solvent systems (water containing 0.1% TFA, water–MeOH = 1:1 containing 0.1% TFA, and MeOH containing 0.1% TFA), **9** was obtained as a brown powder (10.7 mg, 95%). Mp 165–195 °C (dec) (sealed capillary). IR (KBr): 3392, 1683, 1647, 1432, 1276, 1203, 1129 cm^{-1}. ^1H NMR (500 MHz, DMSO-d_6): δ 1.94 (dt, J = 5.9 and 15.3 Hz, 2H), 2.80 (s, 3H), 2.81 (s, 3H), 3.16 (dt, J = 5.7 and 9.0 Hz, 2H), 3.39 (s, 3H), 3.55–3.65 (m, 2H), 3.89 (s, 3H), 6.82 (s, 1H), 6.92 (s, 1H), 6.99 (d, J = 2.0 Hz, 1H), 7.00 (dd, J = 2.0 and 8.0 Hz, 1H), 7.02 (d, J = 7.4 Hz, 1H), 7.13 (s, 1H), 7.14 (s, 1H), 7.24 (d, J = 8.0 Hz, 1H), 9.37 (d, J = 7.4 Hz, 1H), 9.55 (br s, 4H), 11.31 (s, 1H). ^{13}C NMR (126 MHz, DMSO-d_6): δ 23.8, 42.3, 42.4, 54.3, 54.5, 56.2, 65.5, 102.4, 105.4, 107.7, 108.5, 109.7, 110.5, 111.6, 112.1, 113.7, 117.7, 118.5, 122.3, 122.6, 123.9, 127.5, 128.8, 131.2, 131.8, 141.9, 147.4, 147.5, 147.7, 147.7, 148.0, 155.5. HRDARTMS *m*/*z*. Calcd for $C_{32}H_{32}N_3O_7$ [(M−CF_3COO)$^+$]: 570.2240. Found: 570.2239.

*4.5.6. Trifluoroacetic acid salt of 2,3-bis[3-(dimethylamino)propoxy]-11-hydroxy-14-(3-hydroxy-4-methoxyphenyl)-12-methoxy-benzo[7,8]indolizino[3,2-c]quinolin-6(5H)-one (**10**)*

According to the procedure described for the preparation of **7**, **21** (20.0 mg, 27.1 μmol) and $AlCl_3$ (1.0 M solution in nitrobenzene, 200 μL, 0.200 mmol) were reacted. After purification by column chromatography over Sephadex LH-20 using following solvent systems (water containing 0.1% TFA, water–MeOH = 1:1 containing 0.1% TFA, and MeOH containing 0.1% TFA), **10** was obtained as a brown powder (23.1 mg, 97%). Mp 160–200 °C (dec) (sealed capillary). IR (KBr): 3413, 1683, 1432, 1275, 1201, 1130 cm^{-1}. ^1H NMR (500 MHz, DMSO-d_6): δ 1.94 (dt, J = 6.1 and 15.6 Hz, 2H), 2.15 (dt, J = 6.0 and 15.3 Hz, 2H), 2.81 (s, 3H), 2.82 (s, 3H), 2.83 (s, 3H), 2.83 (s, 3H), 3.05–3.13 (m, 2H), 3.19–3.26 (m, 2H), 3.39 (s, 3H), 3.55–3.67 (m, 2H), 3.90 (s, 3H), 4.06 (t, J = 6.0 Hz, 2H), 6.89 (s, 1H), 6.99 (d, J = 2.0 Hz, 1H), 7.01 (dd, J = 2.0 and 8.0 Hz, 1H), 7.02 (s, 1H), 7.06 (d, J = 7.4 Hz, 1H), 7.15 (s, 2H), 7.25 (d, J = 8.0 Hz, 1H), 9.37 (d, J = 7.4 Hz, 1H), 9.42 (br s, 1H), 9.79 (br s, 3H), 11.40 (s,

1H). ^{13}C NMR (126 MHz, DMSO-d_6): δ 23.7, 23.9, 42.3, 42.4, 54.1, 54.4, 54.5, 56.1, 65.6, 65.8, 100.9, 105.4, 107.8, 109.8, 109.9, 110.9, 111.6, 112.3, 113.6, 117.6, 118.4, 122.2, 122.5, 123.9, 127.1, 128.6, 131.3, 131.5, 142.7, 147.5, 147.7, 147.7, 148.1, 148.1, 155.3. HRDARTMS *m/z*. Calcd for $C_{37}H_{43}N_4O_7$ [(M−2CF_3COO−H)$^+$]: 655.3132. Found: 655.3104.

4.6. In vitro kinase assay

Recombinant kinase domains (from amino residues 696 to the C-terminus) of EGFR WT and EGFR T790M/L858R (Cell Signaling Technology) (100 ng) were preincubated with 1–10,000 nM of inhibitors in 25 µL of kinase reaction buffer (120 mM HEPES, pH 7.5, 10 mM $MnCl_2$, 6 µM Na_3VO_4, and 2.5 mM DTT) at 25 °C for 30 min. Then, 25 µL ATP/substrate solution containing 20, 200, or 2,000 µM ATP and 6 µM poly (Glu-Tyr) biotinylated peptide (Cell Signaling Technology) was added to the preincubated samples. The kinase reaction was allowed to proceed at 25 °C for 30 min and terminated by adding 50 µL of 50 mM of EDTA, pH 8.0. Phosphorylation levels were quantified using ELISA, with avidin-coated 96-well plates and an anti-phosphotyrosine antibody (PY20). Unless otherwise mentioned, relative inhibitions were calculated from at least three independent experiments and IC_{50} values were estimated using the mean relative inhibition.[29]

4.7. Docking simulation

Three-dimensional structures of **1**, **5**, **7**, and **10** were built and optimized using the PM3 method implemented in the Spartan 18 package (version 1.4.4).[33] Crystal structure of the EGFR (T790M/L858R/V948R)–gefitinib complex (PDB ID: 4I22)[30] was obtained from the Protein Data Bank. Molecular docking of ligands into the EGFR kinase domain was carried out using the AutoDock Vina program (version 1.1.2)[31] after preparing the ligand and EGFR pdbqt files by the AutoDock Tools program (version 1.5.6).[34] For ligands, the Gasteiger charges were calculated, and all nonpolar hydrogen atoms were merged with the carbon atoms. For EGFR, hydrogen atoms were added to the structure, and the Gasteiger charges were computed. Gefitinib and all the water molecules were removed from the crystal structure of EGFR. The nonpolar hydrogen atoms were merged with the carbon atoms. Leu718, Val726, Lys745, Met790, Leu792, Cys797, Asp800, Glu804, Leu844, Thr854, and Asp855 in EGFR were set as flexible residues. To ensure the inclusion of the ATP-binding site of the EGFR, a 24 × 22 × 22 Å^3 grid box with 1.000 Å grid spacing was used; the grid center coordinates were placed at x = 12.097 Å, y = −12.296 Å, and z = 10.985 Å. The exhaustiveness of the global search and the maximum number of binding modes to be generated were set to 8 and 100. The maximum energy difference between the best and worst binding modes was fixed at 5 kcal/mol. After five docking runs for each ligand, the obtained poses were evaluated using the predicted binding affinity, and the plausible low energy pose for each docked ligand in EGFR was visualized and analyzed using PyMOL (version 2.3.4).[35] These results are shown in **Fig. 4**.

4.8. Proliferation assay

A549 or NCI-H1975 cells (1 × 10^4 cells/well) were cultured in flat-bottom 96-well plates in 150 µL of media containing various concentrations of inhibitors for 72 h. Next, the inhibitor-treated cells were incubated with 0.5 mg/mL MTT in a CO_2 incubator for 4 h, and then 100 µL of 20% SDS was added to each well to dissolve the purple formazan product. The absorption was determined at 570 nm using a spectrophotometer. The relative viability values were calculated from at least three independent experiments. IC_{50} values were estimated using the mean relative viability.[29]

Declaration of Competing Interest

The authors declare that they have no known competing financial interests or personal relationships that could influence the work reported in this paper.

Acknowledgments

This work was supported by JSPS KAKENHI Grant Numbers 26293028, 19K05715, and partially 16H06276 (AdAMS). The author (T.F.) would like to thank the Foundation for Promotion of Cancer Research in Japan and the Naito Foundation for financial support. Some of the results presented herein were obtained using research equipment shared in MEXT Project for promoting public utilization of advanced research infrastructure (Program for supporting introduction of the new sharing system) Grant Number JPMXS0422500320.

Appendix A. Supplementary data

Supplementary data to this article can be found online at https://doi.org/10.1016/j.bmc.2020.00.000.

References

1. da Cunha Santos G, Shepherd FA, Tsao MS. EGFR mutations and lung cancer. *Annu. Rev. Pathol. Mech. Dis.* 2011;6:49–69. https://doi.org/10.1146/annurev-pathol-011110-130206.
2. Shigematsu H, Lin L, Takahashi T, et al. Clinical and biological features associated with epidermal growth factor receptor gene mutations in lung cancers. *J. Natl. Cancer Inst.* 2005;97:339–346. https://doi.org/10.1093/jnci/dji055.
3. Cohen MH, Williams GA, Sridhara R, Chen G, Pazdur R. FDA drug approval summary: gefitinib (ZD1839) (Iressa ®) tablets. *Oncologist* 2003;8:303–306. https://doi.org/10.1634/theoncologist.8-4-303.
4. Dowell J, Minna JD, Kirkpatrick P. Erlotinib hydrochloride. *Nat. Rev. Drug Discov.* 2005;4:13–14. https://doi.org/10.1038/nrd1612.
5. Engelman JA, Janne PA. Mechanisms of acquired resistance to epidermal growth factor receptor tyrosine kinase inhibitors in non–small cell lung cancer. *Clin. Cancer Res.* 2008;14:2895–2899. https://doi.org/10.1158/1078-0432.CCR-07-2248.
6. The T790M secondary mutation restore the ATP affinity of the mutant to near EGFR WT levels ($K_{m[ATP]}$ values for EGFR WT, L858R, and T790M/L858R mutants are 5.2, 148, and 8.4 µM). Please see: Yun C-H, Mengwasser KE, Toms AV, et al. The T790M mutation in EGFR kinase causes drug resistance by increasing the affinity for ATP. *Proc. Natl. Acad. Sci.* 2008;105:2070–2075. https://doi.org/10.1073/pnas.0709662105.
7. Li D, Ambrogio L, Shimamura T, et al. BIBW2992, an irreversible EGFR/HER2 inhibitor highly effective in preclinical lung cancer models. *Oncogene.* 2008;27:4702–4711. https://doi.org/10.1038/onc.2008.109.
8. Engelman JA, Zejnullahu K, Gale C-M, et al. PF00299804, an irreversible pan-ERBB inhibitor, is effective in lung cancer models with EGFR and ERBB2 mutations that are resistant to gefitinib. *Cancer Res.* 2007;67:11924–11932. https://doi.org/10.1158/0008-5472.CAN-07-1885.
9. Minami Y, Shimamura T, Shah K, et al. The major lung cancer-derived mutants of ERBB2 are oncogenic and are associated with sensitivity to the irreversible EGFR/ERBB2 inhibitor HKI-272. *Oncogene.* 2007;26:5023–5027. https://doi.org/10.1038/sj.onc.1210292.
10. Kim Y, Ko J, Cui Z, et al. The EGFR T790M mutation in acquired resistance to an irreversible second-generation EGFR inhibitor. *Mol. Cancer Ther.* 2012;11:784–791. https://doi.org/10.1158/1535-7163.MCT-11-0750.
11. Janne PA, Schellens JH, Engelman JA, et al. Preliminary activity and safety results from a phase I clinical trial of PF-00299804, an irreversible pan-HER inhibitor, in patients (pts) with NSCLC. *J. Clin. Oncol.* 2008;26:8027. https://doi.org/10.1200/jco.2008.26.15_suppl.8027.
12. Sequist LV, Besse B, Lynch TJ, et al. Neratinib, an irreversible pan-ErbB receptor tyrosine kinase inhibitor: results of a phase II trial in

patients with advanced non–small-cell lung cancer. *J. Clin. Oncol.* 2010;28:3076–3083. https://doi.org/10.1200/JCO.2009.27.9414.
13. Zhou W, Ercan D, Chen L, et al. Novel mutant-selective EGFR kinase inhibitors against EGFR T790M. *Nature.* 2009;462:1070–1074. https://doi.org/10.1038/nature08622.
14. Walter AO, Sjin RTT, Haringsma HJ, et al. Discovery of a mutant-selective covalent inhibitor of EGFR that overcomes T790M-mediated resistance in NSCLC. *Cancer Discov.* 2013;3:1404–1415. https://doi.org/10.1158/2159-8290.CD-13-0314.
15. Cross DAE, Ashton SE, Ghiorghiu S, et al. AZD9291, an irreversible EGFR TKI, overcomes T790M-mediated resistance to EGFR inhibitors in lung cancer. *Cancer Discov.* 2014;4:1046–1061. https://doi.org/10.1158/2159-8290.CD-14-0337.
16. Soria J-C, Ohe Y, Vansteenkiste J, et al. Osimertinib in untreated EGFR-mutated advanced non–small-cell lung cancer. *N. Engl. J. Med.* 2018;378:113–125. https://doi.org/10.1056/NEJMoa1713137.
17. Thress KS, Paweletz CP, Felip E, et al. Acquired EGFR C797S mutation mediates resistance to AZD9291 in non–small cell lung cancer harboring EGFR T790M. *Nat. Med.* 2015;21:560–562. https://doi.org/10.1038/nm.3854.
18. Baunbæk D, Trinkler N, Ferandin Y, et al. Anticancer alkaloid lamellarins inhibit protein kinases. *Mar. Drugs.* 2008;6:514–527. https://doi.org/10.3390/md20080026.
19. Yoshida K, Itoyama R, Yamahira M, et al. Synthesis, resolution, and biological evaluation of atropisomeric (a*R*)- and (a*S*)-16-methyllamellarins N: unique effects of the axial chirality on the selectivity of protein kinases inhibition. *J. Med. Chem.* 2013;56:7289–7301. https://doi.org/10.1021/jm400719y.
20. Fukuda T, Umeki T, Tokushima K, et al. Design, synthesis, and evaluation of A-ring-modified lamellarin N analogues as noncovalent inhibitors of the EGFR T790M/L858R mutant. *Bioorg. Med. Chem.* 2017;25:6563–6580. https://doi.org/10.1016/j.bmc.2017.10.030.
21. Boonya-udtayan S, Yotapan N, Woo C, Bruns CJ., Ruchirawat S, Thasana N. Synthesis and biological activities of azalamellarins. *Chem. - An Asian J.* 2010;5:2113–2123. https://doi.org/10.1002/asia.201000237.
22. Theppawong A, Ploypradith P, Chuawong P, Ruchirawat S, Chittchang M. Facile and divergent synthesis of lamellarins and lactam-containing derivatives with improved drug likeness and biological activities. *Chem. - An Asian J.* 2015;10:2631–2650. https://doi.org/10.1002/asia.201500611.
23. Komatsubara M, Umeki T, Fukuda T, Iwao M. Modular synthesis of lamellarins via regioselective assembly of 3,4,5-differentially arylated pyrrole-2-carboxylates. *J. Org. Chem.* 2014;79:529–537. https://doi.org/10.1021/jo402181w.
24. Ikegashira K, Oka T, Hirashima S, et al. Discovery of conformationally constrained tetracyclic compounds as potent hepatitis C virus NS5B RNA polymerase inhibitors. *J. Med. Chem.* 2006;49:6950–6953. https://doi.org/10.1021/jm0610245.
25. Jacquemard U, Bénéteau V, Lefoix M, Routier S, Mérour J-Y, Coudert G. Mild and selective deprotection of carbamates with Bu_4NF. *Tetrahedron.* 2004; 60:10039–10047. https://doi.org/10.1016/j.tet.2004.07.071.
26. Fujikawa N, Ohta T, Yamaguchi T, Fukuda T, Ishibashi F, Iwao, M. Total synthesis of lamellarins D, L, and N. *Tetrahedron.* 2006;62:594–604. https://doi.org/10.1016/j.tet.2005.10.014.
27. Kamiyama H, Kubo Y, Sato H, et al. Synthesis, structure–activity relationships, and mechanism of action of anti-HIV-1 lamellarin α 20-sulfate analogues. *Bioorg. Med. Chem.* 2011;19:7541–7550. https://doi.org/10.1016/j.bmc.2011.10.030.
28. Banwell MG, Flynn BL, Stewart SG. Selective cleavage of isopropyl aryl ethers by aluminum trichloride. *J. Org. Chem.* 1998;63:9139–9144. https://doi.org/10.1021/jo9808526.
29. Nishiya N, Sakamoto Y, Oku Y, Nonaka T, Uehara Y. JAK3 inhibitor VI is a mutant specific inhibitor for epidermal growth factor receptor with the gatekeeper mutation T790M. *World J. Biol. Chem.* 2015;6:409–418. https://doi.org/10.4331/wjbc.v6.i4.409.
30. Gajiwala KS, Feng J, Ferre R, et al. Insights into the aberrant activity of mutant EGFR kinase domain and drug recognition. *Structure*. 2013;21:209–219. https://doi.org/10.1016/j.str.2012.11.014.
31. Trott O, Olson AJ. AutoDock Vina: improving the speed and accuracy of docking with a new scoring function, efficient optimization, and multithreading. *J. Comput. Chem.* 2010;31:455–461. https://doi.org/10.1002/jcc.21334.
32. Gaillard T. Evaluation of AutoDock and AutoDock Vina on the CASF-2013 benchmark. *J. Chem. Inf. Model.* 2018;58:1697–1706. https://doi.org/10.1021/acs.jcim.8b00312.
33. Spartan 18, version 1.4.4; Wavefunction, Inc. https://www.wavefun.com.
34. Morris GM, Huey R, Lindstrom W, et al. AutoDock4 and AutoDockTools4: automated docking with selective receptor flexibility. *J. Comput. Chem.* 2009;30:2785–2791. https://doi.org/10.1002/jcc.21256.
35. The PyMOL Molecular Graphics System, version 2.3.4; Schrödinger, LLC. https://pymol.org.